



IEEE Custom Integrated Circuits Conference

Clocking for Serial Links

Saurabh Saxena

Department of Electrical Engineering

Indian Institute of Technology Madras

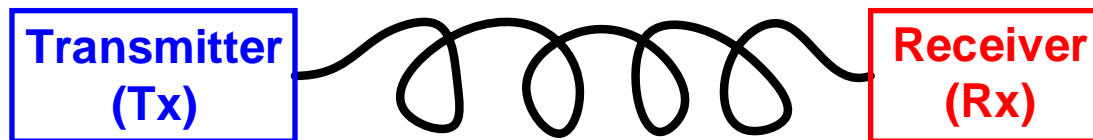
24th April, 2022



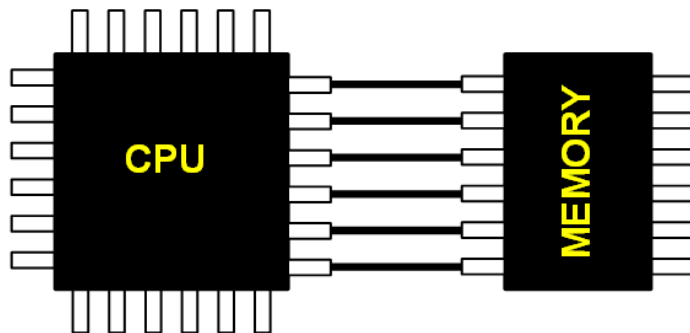
IEEE
SOLID-STATE
CIRCUITS SOCIETY™



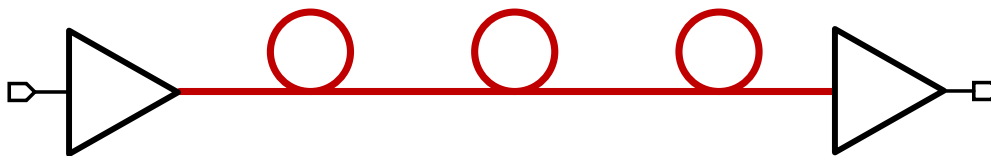
Serial Link Applications



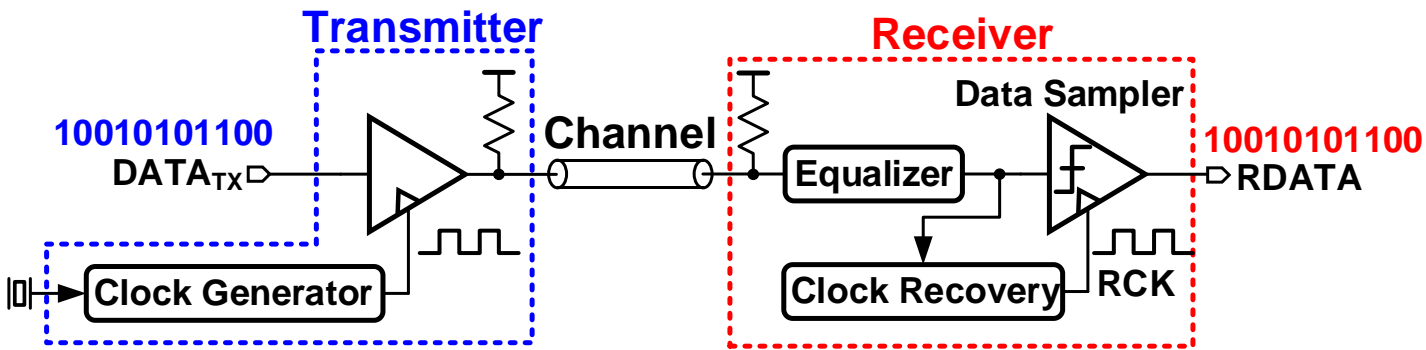
Chip-to-chip
Electrical link



Optical link

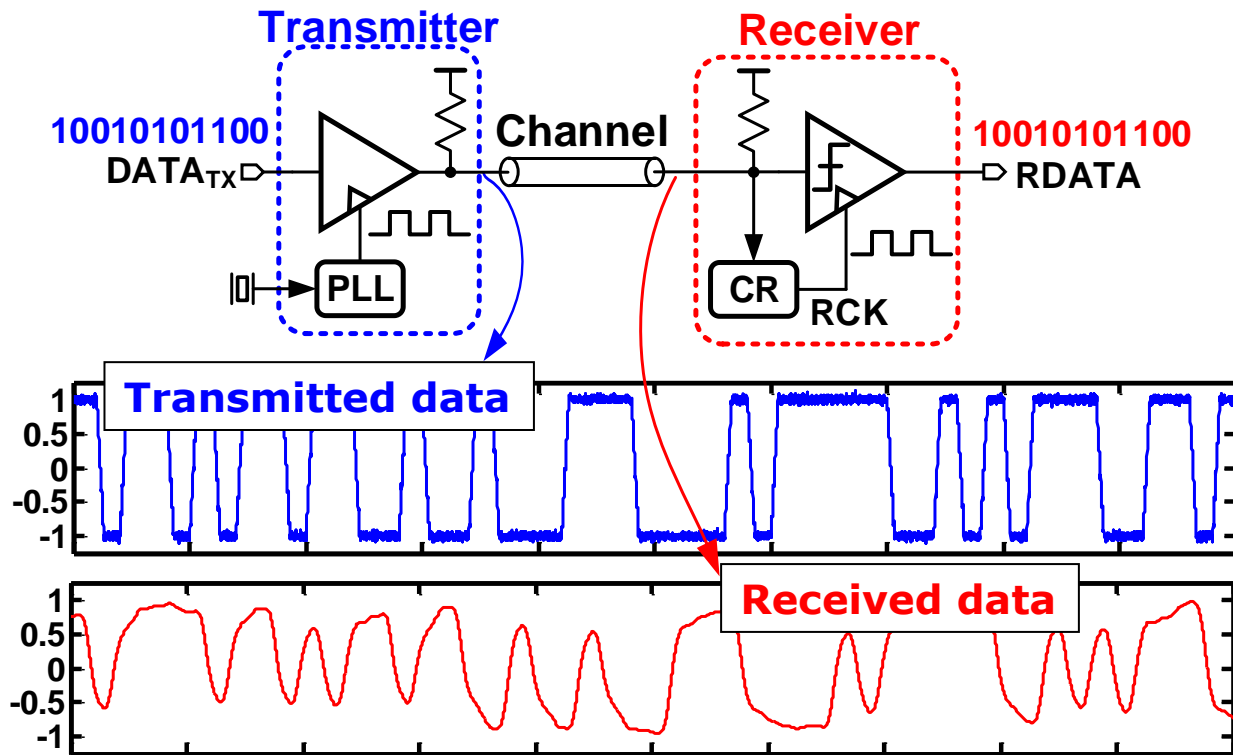


Serial Link Components

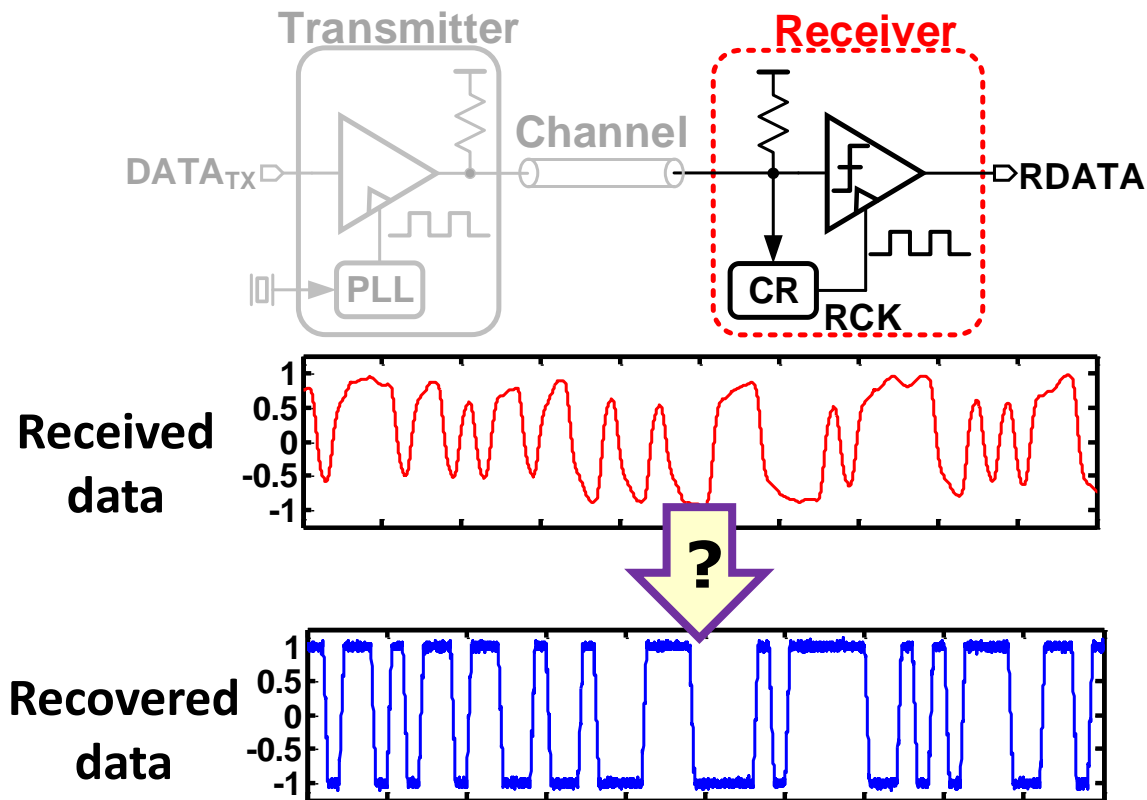


- ❑ Transmitter
- ❑ Channel
- ❑ Receiver
- ❑ Serial links with embedded clock \Rightarrow RCK is recovered from received data
- ❑ Clock Recovery (CR) + Data sampler = CDR

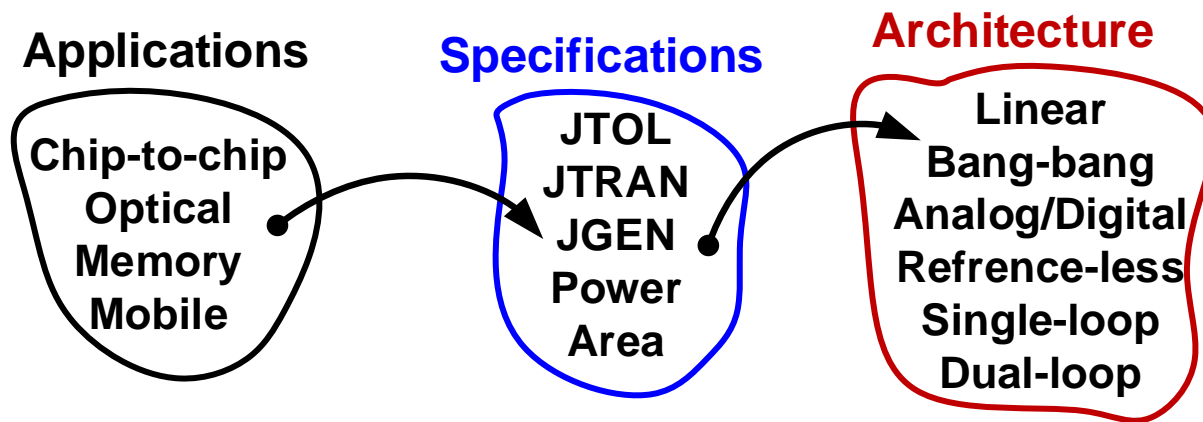
Serial Link Waveforms



Clock and Data Recovery



Goals



- ❑ Map application requirements to CDR specifications
- ❑ Optimal architecture choice based on CDR specifications
 - Exposure to different CDR architectures
 - Develop intuition for design tradeoffs
 - Awareness to practical considerations

Overview

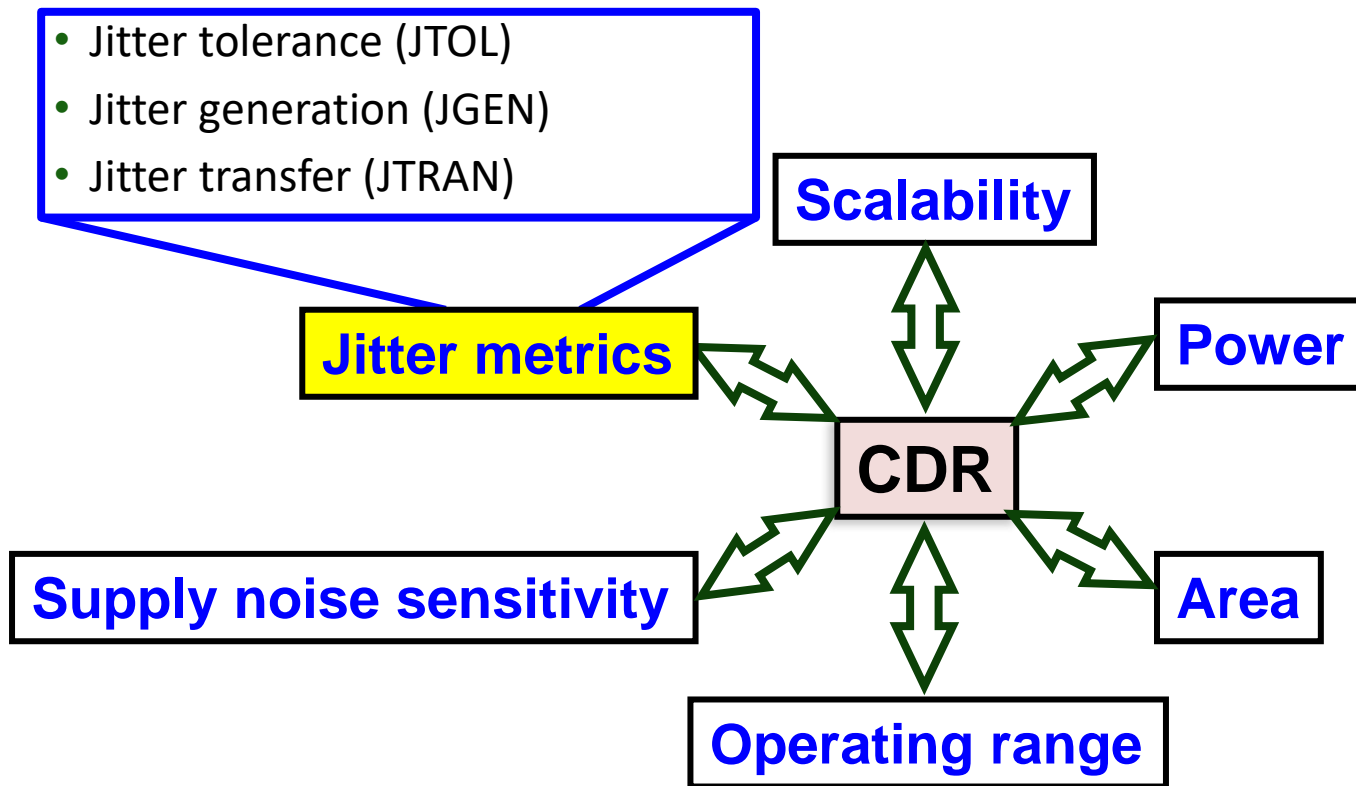
- ❑ Performance metrics

- ❑ Basic architectures
 - Linear/Bang-bang
 - Digital
 - Hybrid

- ❑ Application-specific CDRs
 - Multi-lane chip-to-chip links
 - Repeaters for optical links and active cables

- ❑ Frequency detectors

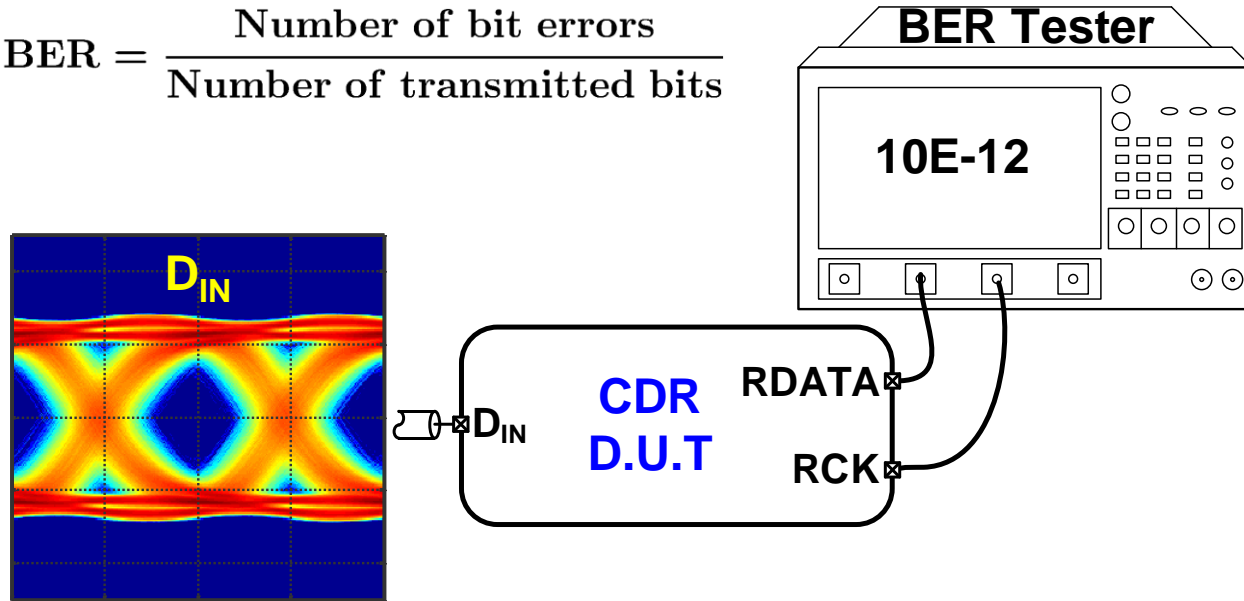
CDR Performance Metrics



Jitter Tolerance (JTOL)

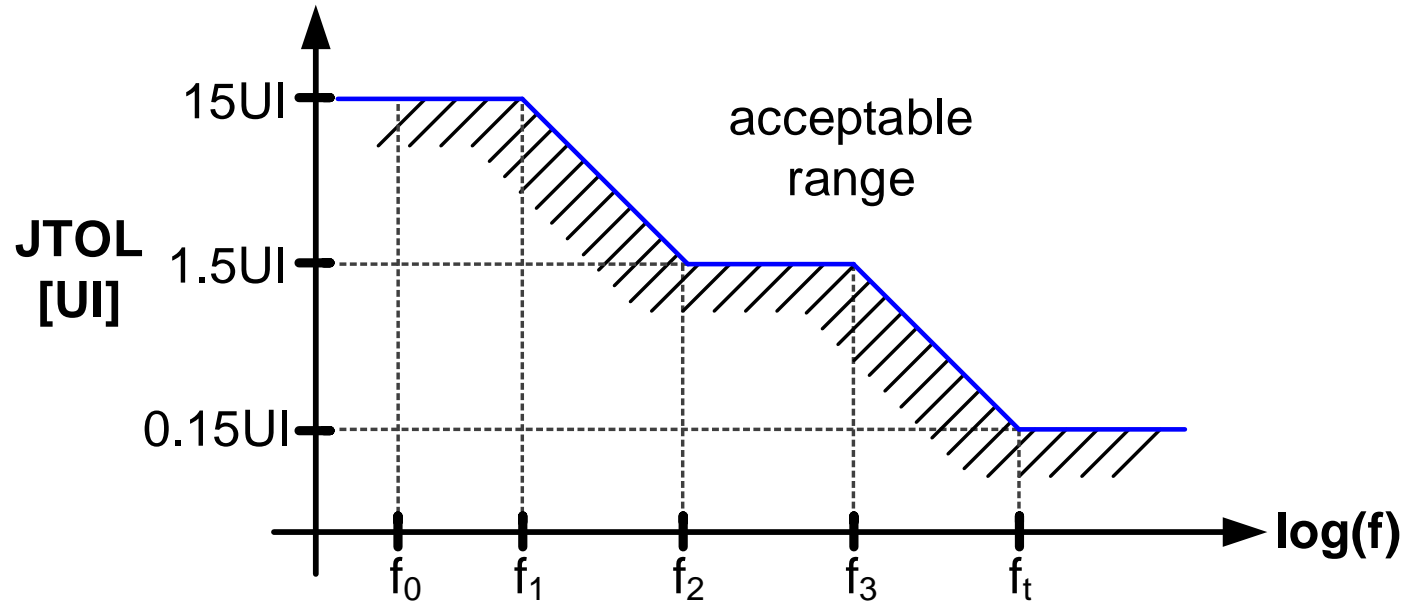
- Maximum tolerable peak-to-peak sinusoidal input jitter for a given BER

$$\text{BER} = \frac{\text{Number of bit errors}}{\text{Number of transmitted bits}}$$



- JTOL varies with frequency of the sinusoidal input

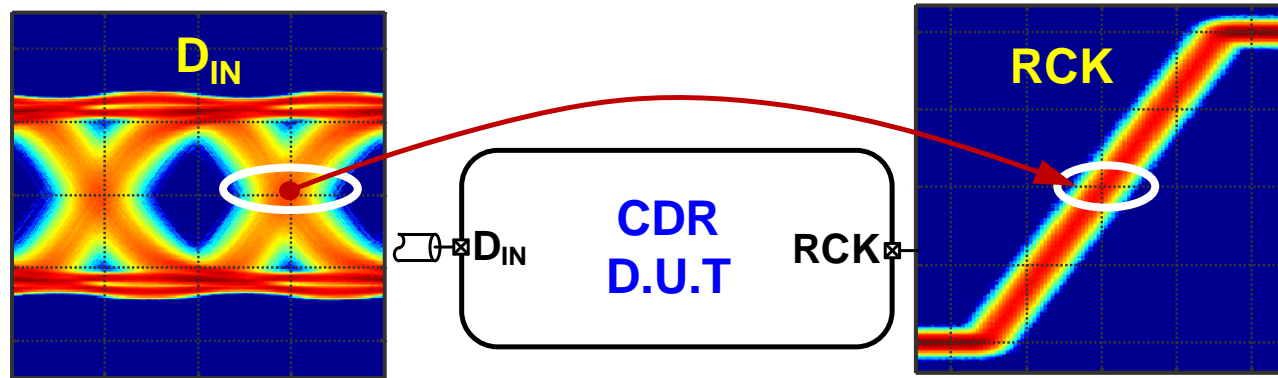
JTOL Mask



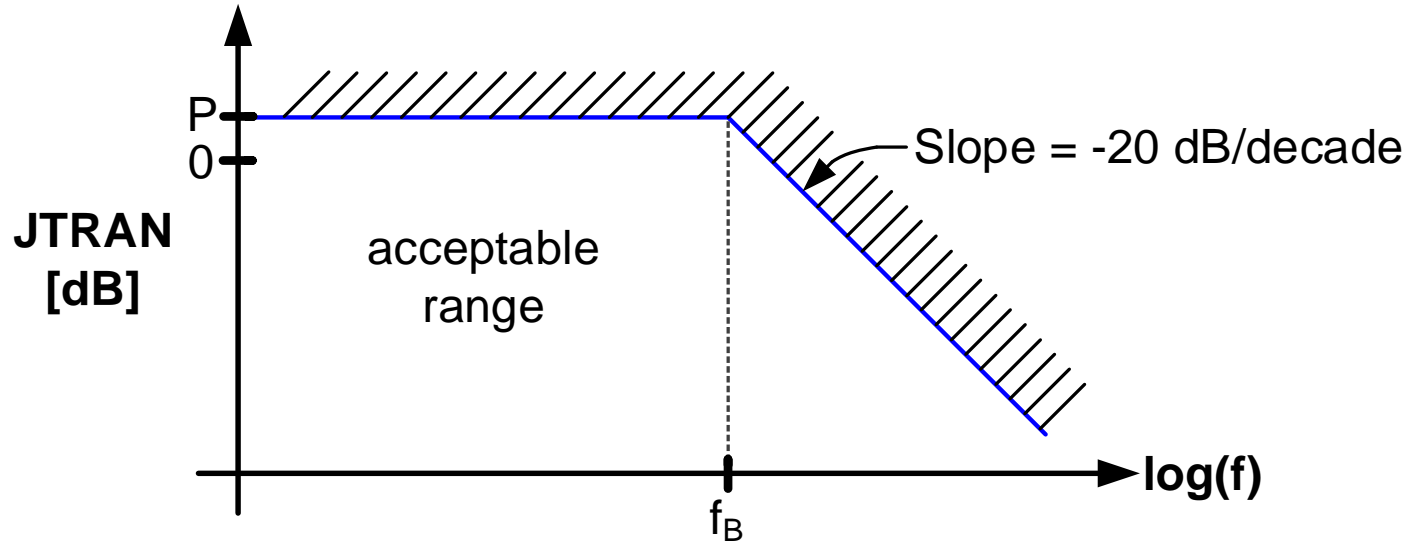
- Increase data input sinusoidal jitter until BER exceeds target

Jitter Transfer (JTRAN)

- Amount of jitter attenuation provided by CDR



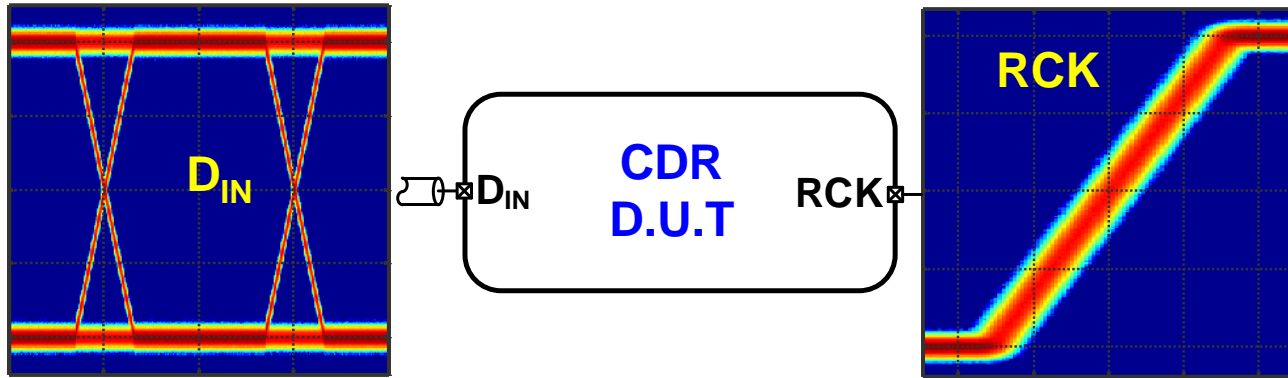
JTRAN Mask



- ❑ Modulate data input with sinusoidal jitter & measure resulting output jitter

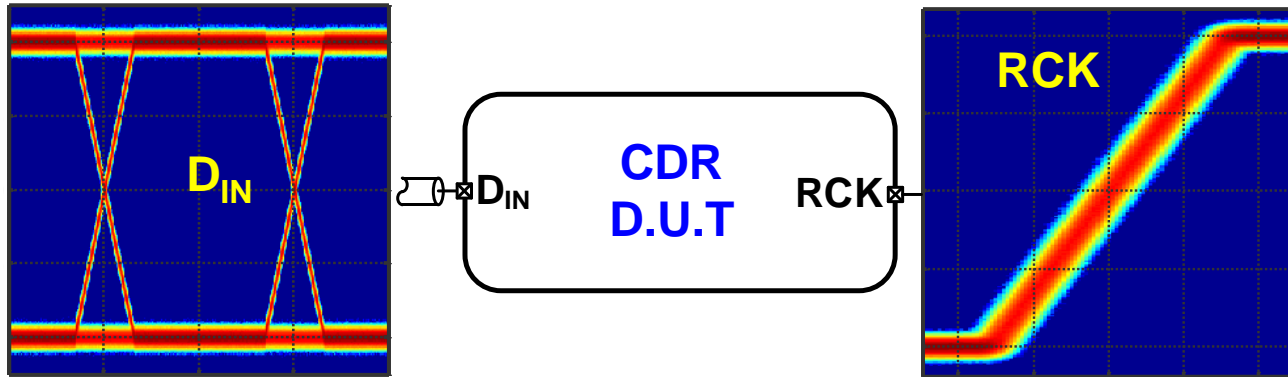
Jitter Generation (JGEN)

- Amount of output jitter when fed with clean data



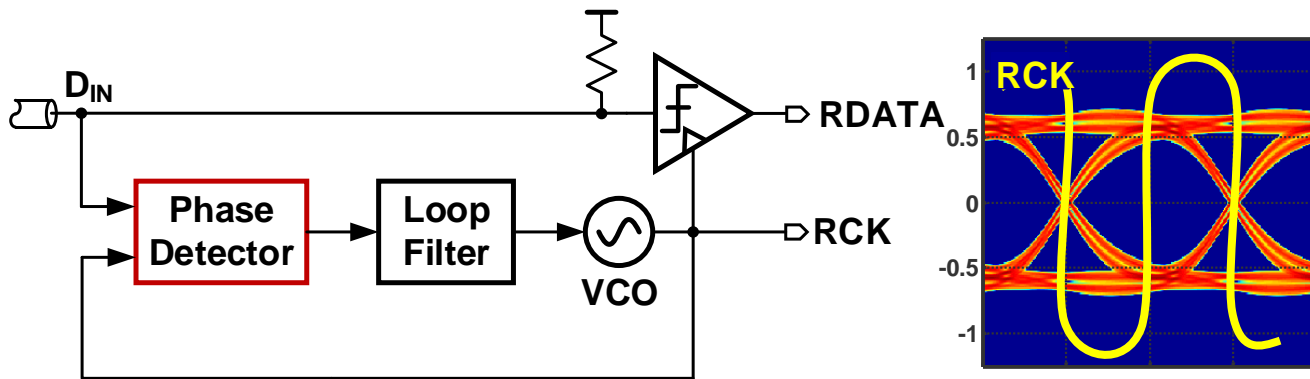
Jitter Generation (JGEN)

- Amount of output jitter when fed with clean data



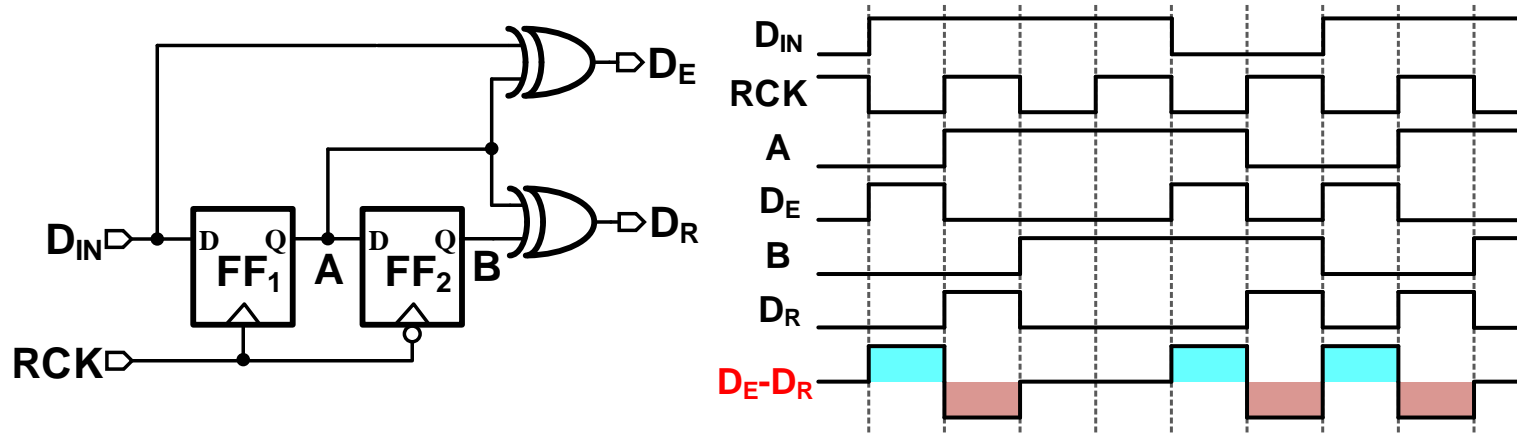
Need: Design CDR for given JTOL corner frequency, JTRAN BW, and JGEN

Phase Locked Loop based CDR



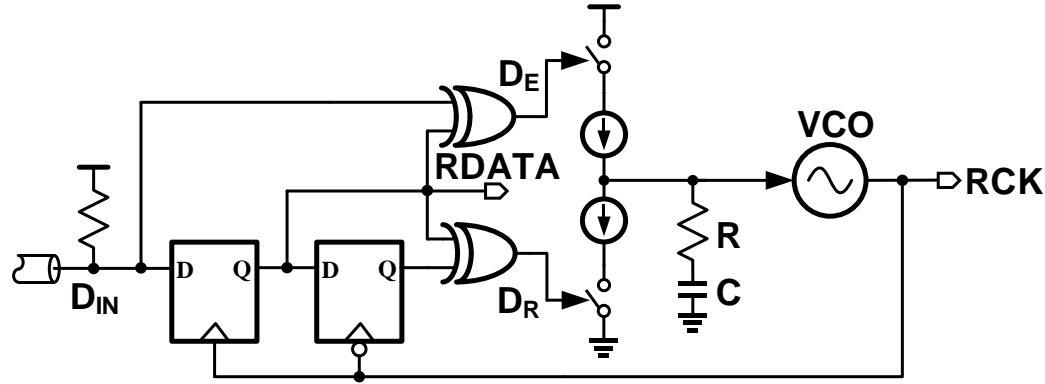
- ❑ Building blocks similar to a PLL
- ❑ Phase detector should tolerate missing transitions
- ❑ Negative edge of recovered clock locks to data edge
- ❑ Positive edge samples data in the middle of the eye

Linear (Hogge) Phase Detector^[1]



- ❑ Error output ($D_E - D_R$) is difference of 2 pulses
 - Pulse width of D_E is proportional to phase error
 - Pulse width of D_R is fixed and is equal to $T_{RCK}/2$
- ❑ Area under $D_E - D_R$ is proportional to phase error
 - Area is zero when RCK is aligned with D_{IN}

CDR Using Hogge Phase Detector



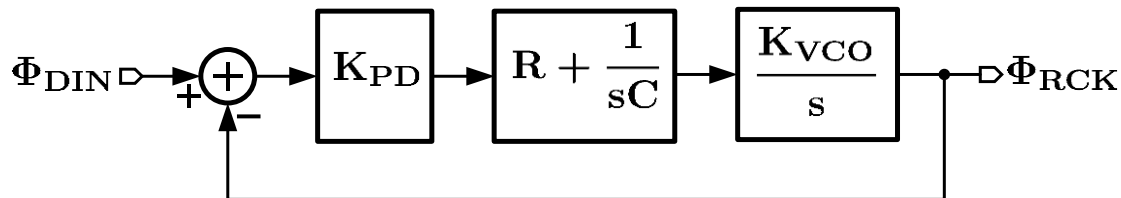
□ Type-II response

- 2 integrators – one in the loop filter and the other is VCO

□ Zero static phase offset (ideally)

- CP output should be zero in steady state
- Implies input phase error = 0

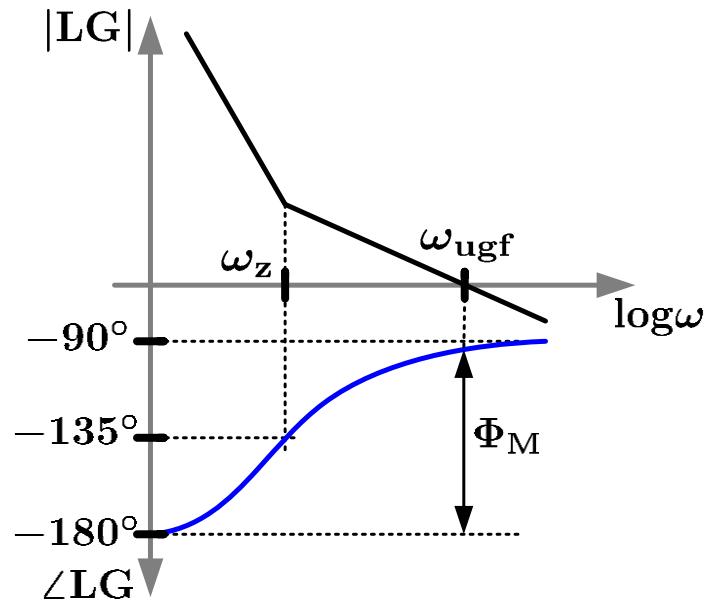
Choosing Loop Parameters



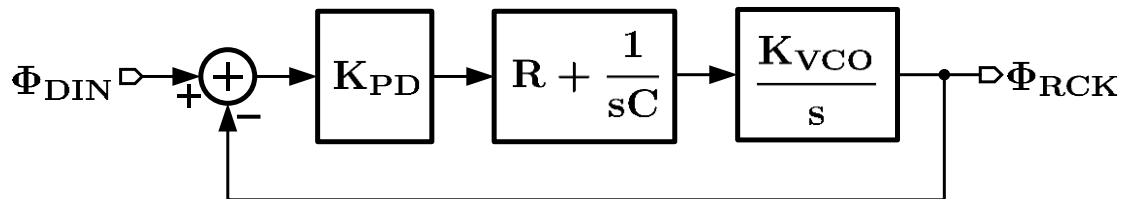
$$LG(s) = K_{PD} \cdot \left(R + \frac{1}{sC} \right) \cdot \frac{K_{VCO}}{s}$$

$$\omega_z = \frac{1}{RC}, \quad \omega_{p1} = 0, \quad \omega_{p2} = 0$$

$$\Phi_M = \arctan \left(\frac{\omega_{ugf}}{\omega_z} \right)$$



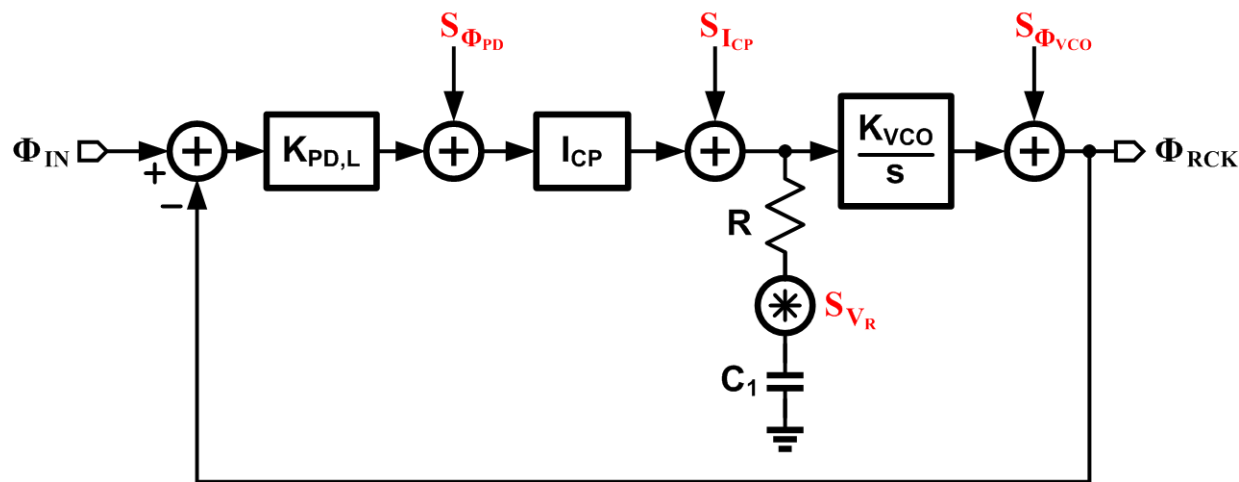
Jitter Transfer Function (JTRAN)



$$\begin{aligned}
 H_{\text{JTRAN}}(s) &= \frac{\Phi_{\text{RCK}}(s)}{\Phi_{\text{DIN}}(s)} \\
 &= \frac{1 + sRC}{1 + sRC + s^2 \cdot \frac{C}{K_{\text{VCO}}K_{\text{PD}}}} \\
 &\equiv \frac{1 + s/\omega_z}{(1 + s/\omega_{\text{PL}})(1 + s/\omega_{\text{PH}})}
 \end{aligned}
 \left. \begin{array}{l} \omega_z = 1/RC \\ \omega_{\text{PL}} \approx 1/RC \\ \omega_{\text{PH}} \approx K_{\text{VCO}} \cdot K_{\text{PD}} \cdot R \end{array} \right\}$$

$\text{JTRAN BW} = \omega_{-3\text{dB}} \approx \omega_{\text{PH}} \approx K_{\text{VCO}} \cdot K_{\text{PD}} \cdot R$

Phase Noise Analysis of Linear CDR (I)



$S_{\Phi_{PD}}$: PD's noise PSD

$S_{I_{CP}}$: Charge-pump's noise PSD

S_{V_R} : Resistor's noise PSD

$S_{\Phi_{VCO}}$: VCO's noise PSD

$$\square \text{NTF}_{IN} = \frac{LG}{1 + LG}$$

$$\square \text{NTF}_{PD} = \frac{1}{K_{PD,L}} \times \frac{LG}{1 + LG}$$

$$\square \text{NTF}_{CP} = \frac{1}{K_{PD,L} I_{CP}} \times \frac{LG}{1 + LG}$$

$$\square \text{NTF}_R = \frac{K_{VCO}}{s} \times \frac{1}{1 + LG}$$

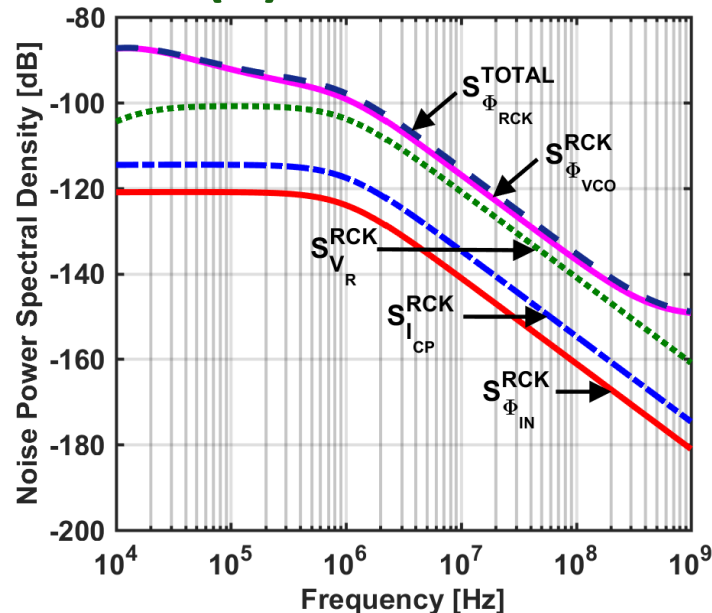
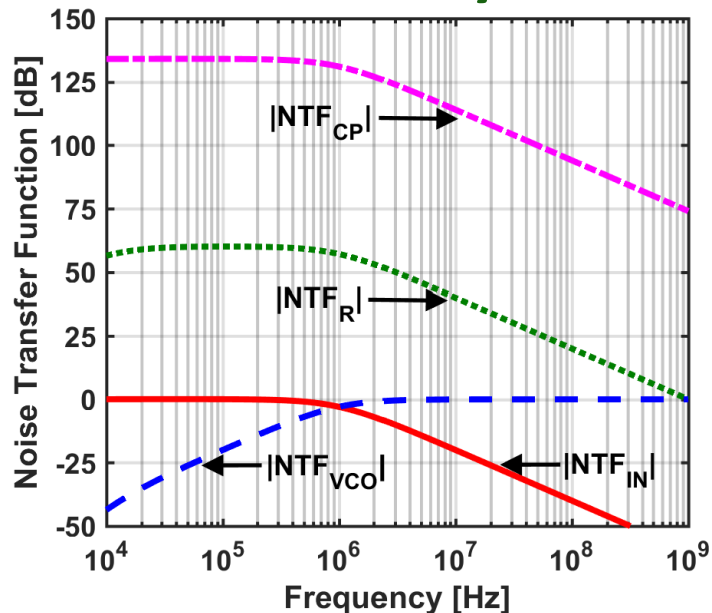
$$\square \text{NTF}_{VCO} = \frac{1}{1 + LG}$$

$$\square J_{GEN} = \frac{T_{RCK}}{2\pi} \sqrt{\int_0^\infty S_{\Phi_{RCK}}^{Total} df}$$

where $S_{\Phi_{RCK}}^{Total} = \sum S_i \times |\text{NTF}_i|^2$

S_i : i^{th} noise source

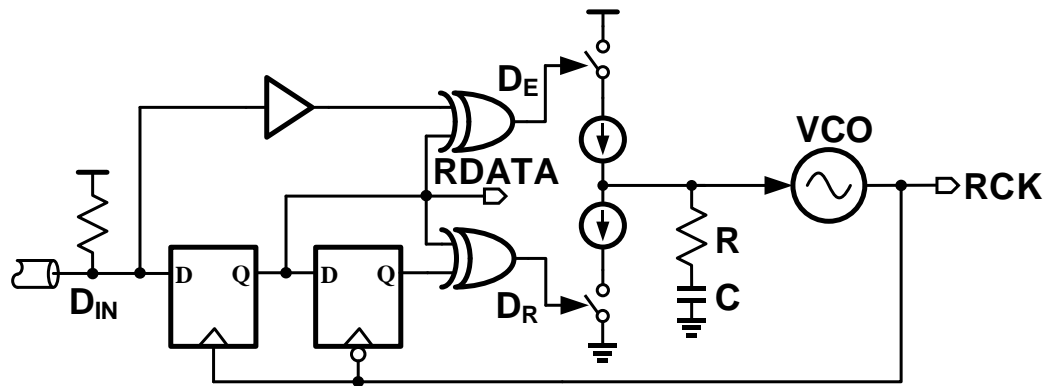
Phase Noise Analysis of Linear CDR (II)



Design Example:

- DR = 2.5Gb/s, $f_{RCK} = 2.5\text{GHz}$, $K_{VCO} = 2\pi \text{ Grad/s/V}$, Phase margin = 85° , JTRAN BW < 1MHz
- $I_{CP} = 1.26 \mu\text{A}$, $R = 5 \text{ k}\Omega$, $C_1 = 2.76 \text{ nF}$
- VCO's noise dominates in low JTRAN BW designs

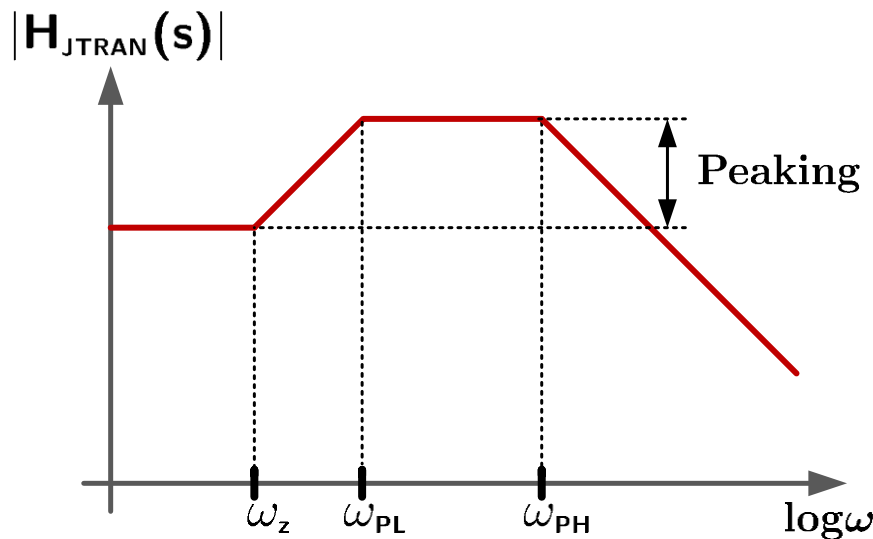
Linear CDR Drawbacks



- ❑ JTRAN peaking vs large loop filter capacitor
- ❑ Coupled JTRAN and JTOL
- ❑ Hogge PD non-idealities

Jitter Peaking^[2]

□ Zero in feed-forward path → inevitable peaking



$$H_{JTRAN} = \frac{1 + sRC}{1 + sRC + s^2 \cdot \frac{C}{K_{VCO}K_{PD}}}$$

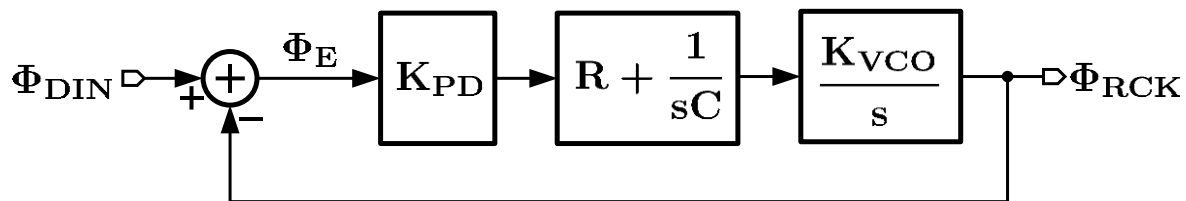
$$\omega_z = 1/RC$$

$$\omega_{PL} \approx 1/RC$$

$$\omega_{PH} \approx K_{VCO} \cdot K_{PD} \cdot R$$

$$\text{Jitter Peaking [dB]} \approx \frac{8.686}{K_{VCO} K_{PD} CR^2} \approx \frac{8.686}{\omega_{-3dB} CR} = \frac{8.686 \omega_z}{\omega_{-3dB}}$$

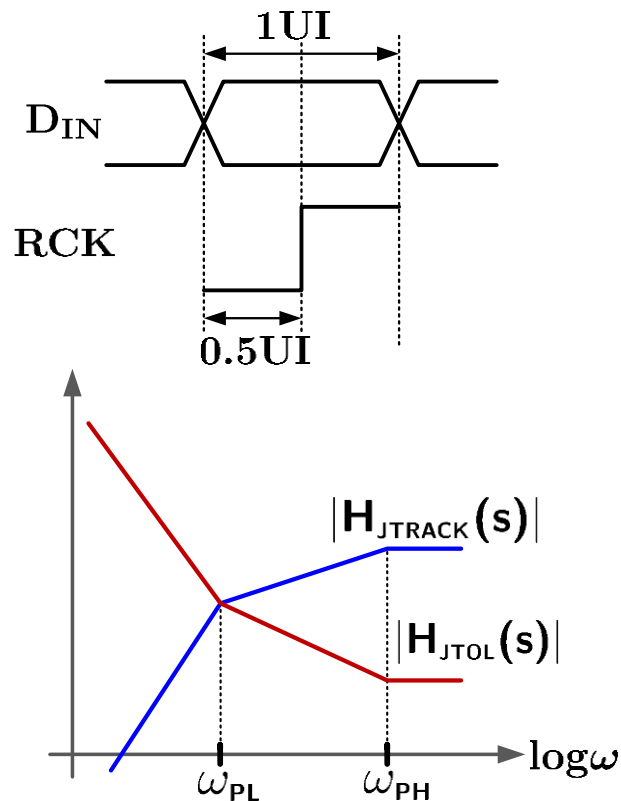
Jitter Tracking



$$\begin{aligned}
 H_{JTRACK}(s) &= \frac{\Phi_E(s)}{\Phi_{DIN}(s)} = \frac{1}{1 + LG(s)} \\
 &= \frac{s^2 \cdot \frac{C}{K_{VCO}K_{PD}}}{1 + sRC + s^2 \cdot \frac{C}{K_{VCO}K_{PD}}} \\
 &\equiv \frac{s^2 / \omega_{PL}\omega_{PH}}{(1 + s/\omega_{PL})(1 + s/\omega_{PH})}
 \end{aligned}$$

$$JTRACK\ BW = \omega_{-3dB} \approx \omega_{PH} \approx K_{VCO} \cdot K_{PD} \cdot R$$

Jitter Tolerance (JTOL)



$$|\Phi_E| < 0.5 UI$$

$$\Phi_{DIN} \times H_{JTRACK}(s) < 0.5 UI$$

$$\Rightarrow \Phi_{DIN} < \frac{0.5 UI}{H_{JTRACK}(s)}$$

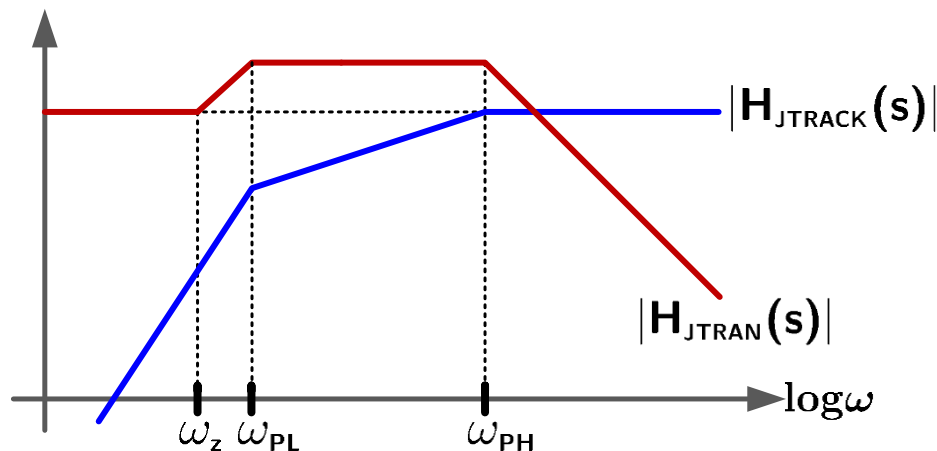
$$H_{JTOL}(s) = \frac{0.5}{H_{JTRACK}(s)}$$

$$H_{JTOL}(s) = \frac{0.5 (1 + s/\omega_{PL}) (1 + s/\omega_{PH})}{s^2/\omega_{PL}\omega_{PH}}$$

Coupled JTRAN/JTOL Behavior

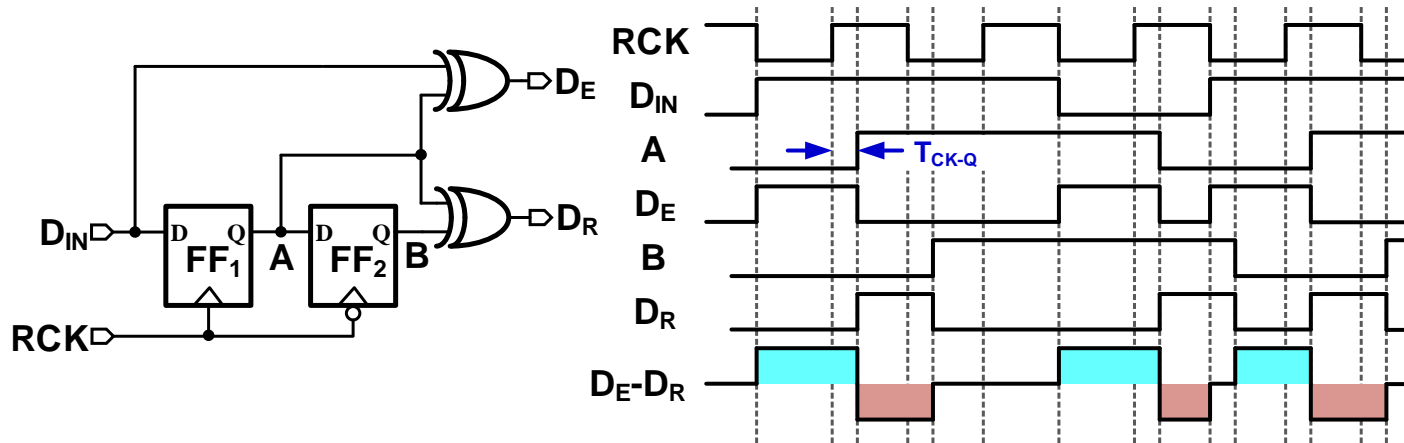
$$H_{JTRAN}(s) = \frac{1 + sRC}{1 + sRC + s^2 \cdot \frac{C}{K_{VCO}K_{PD}}}$$

$$H_{JTRACK}(s) = \frac{s^2 \cdot \frac{C}{K_{VCO}K_{PD}}}{1 + sRC + s^2 \cdot \frac{C}{K_{VCO}K_{PD}}}$$



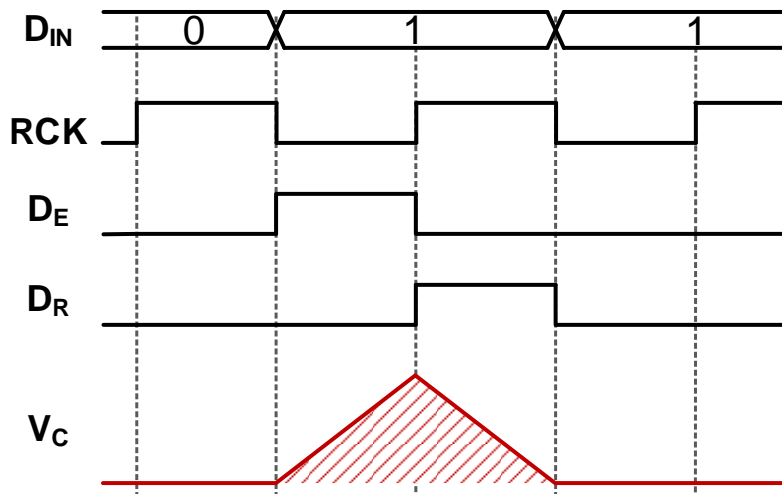
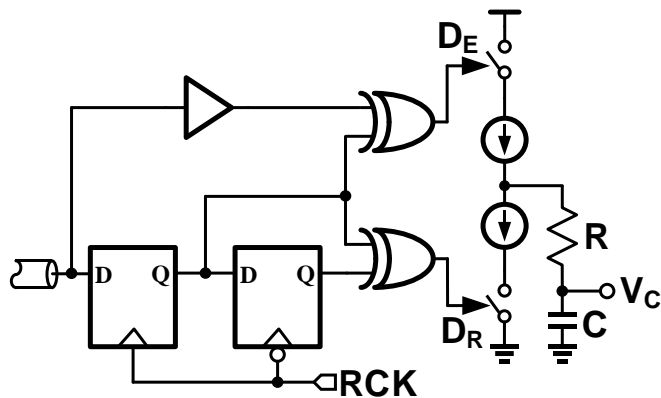
□ Both JTRAN and JTOL are governed by ω_{PH}

Hogge PD Non-idealities: Offset [2]



- ❑ FF_1 clock-to-Q delay introduces phase offset

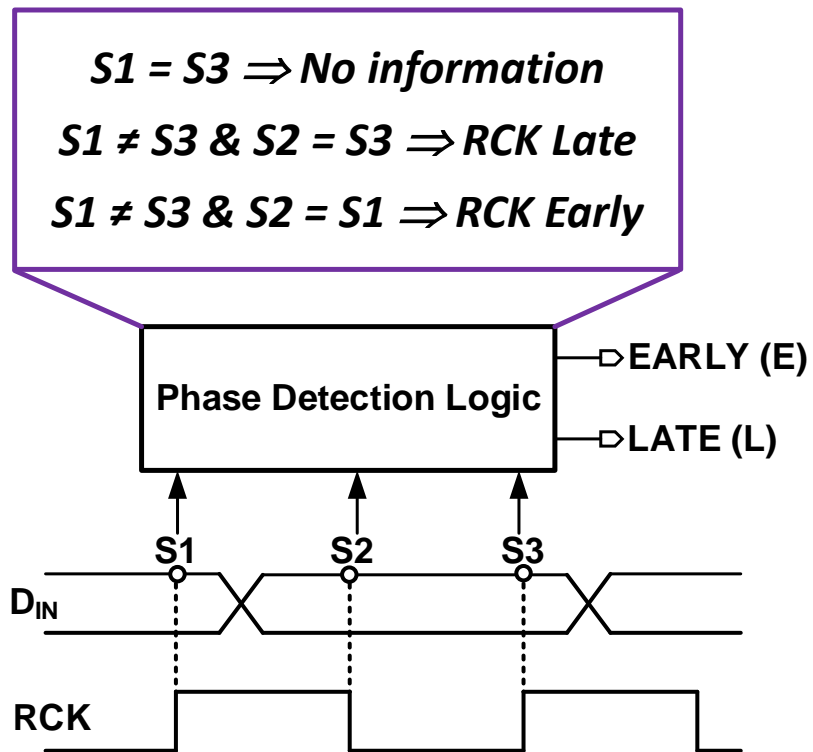
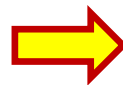
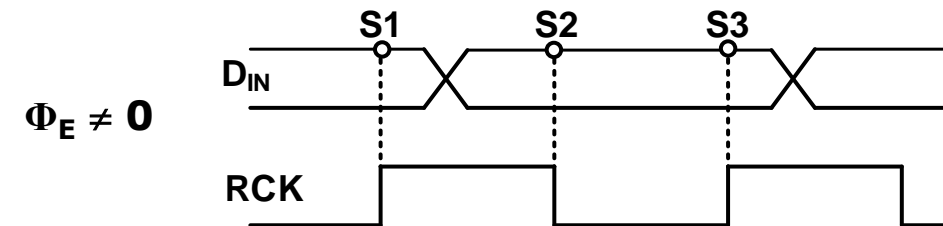
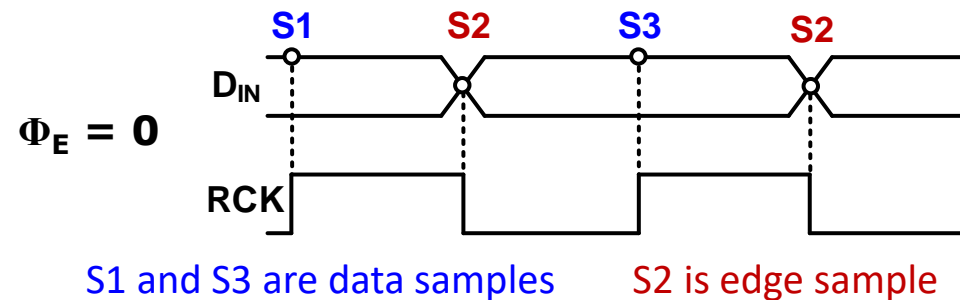
Hogge PD Non-idealities: DDJ^[2]



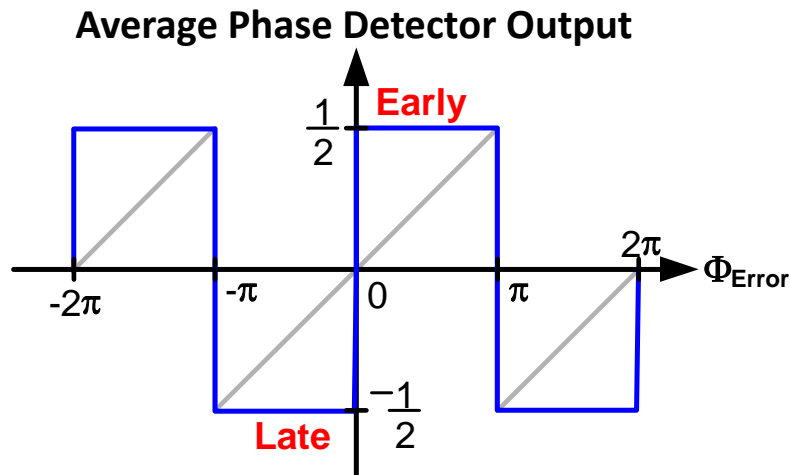
- D_E/D_R pulses not aligned in time
 - “Tri-wave” on V_C causes Data Dependent Jitter (DDJ)

- See [2] for modified Hogge PD to mitigate offset and DDJ

Bang-Bang Phase Detector (BBPD)^[3]



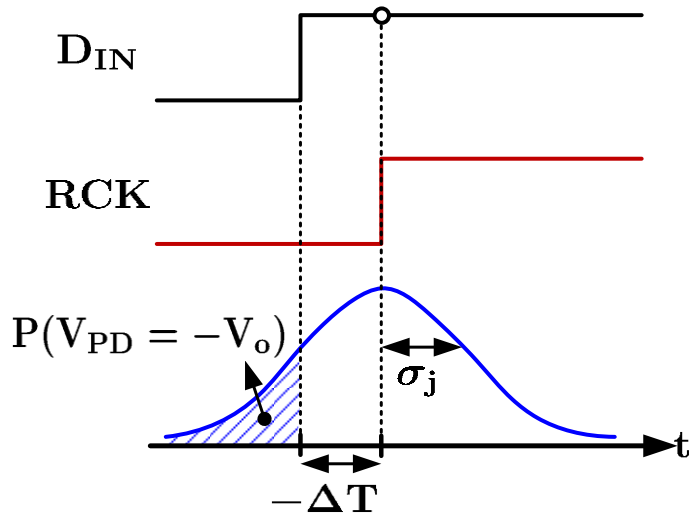
BBPD Characteristics: w/o Jitter



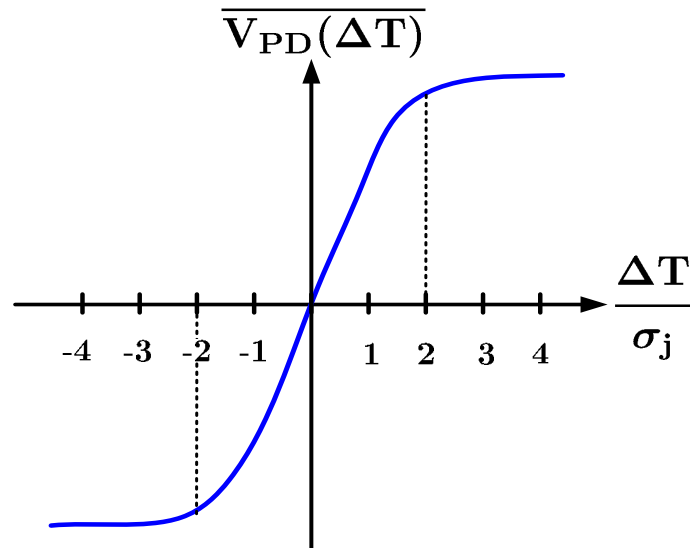
Useful range : $\pm\pi$

Gain $K_{\text{PD}}|_{\Delta T=0} = \infty$

BBPD Characteristics: w/ Jitter^[4]



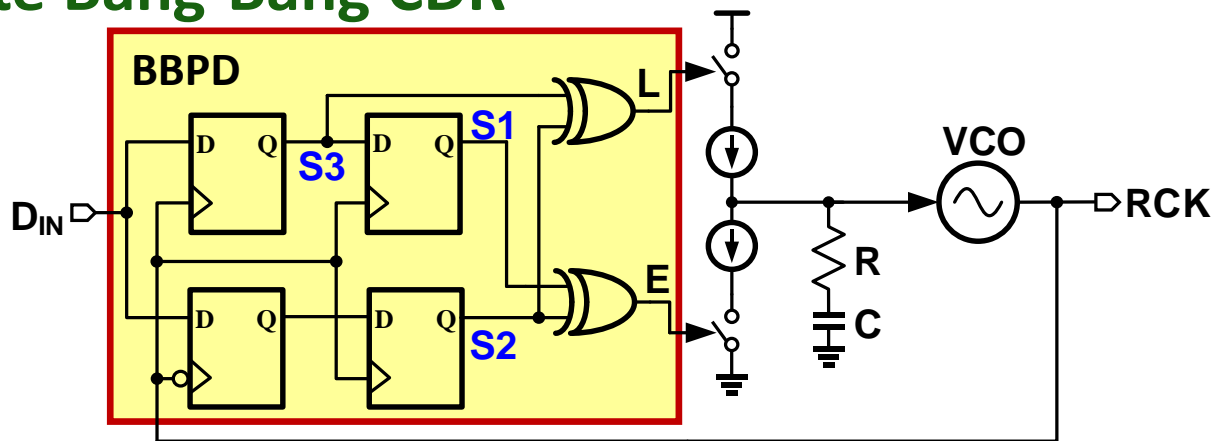
$$\overline{V_{PD}(\Delta T)} = -V_o \cdot P(V_{PD} = -V_o) + V_o \cdot P(V_{PD} = V_o)$$



$$\overline{V_{PD}(\Delta T)} = \frac{2V_o}{\sqrt{2\pi}} \int_0^{\Delta T/\sigma_j} e^{-y^2} dy$$

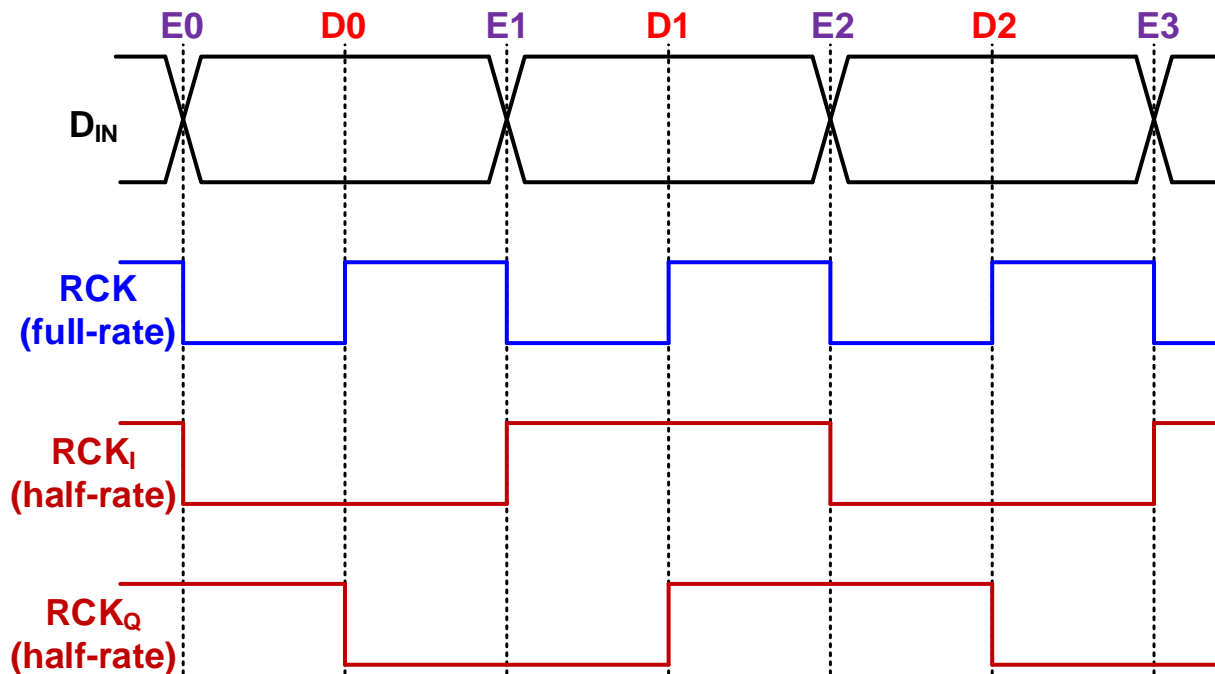
$$K_{PD} = \frac{d\overline{V_{PD}(\Delta T)}}{d\Delta T} = \frac{2V_o}{\sqrt{2\pi}\sigma_j} e^{\left(-\frac{\Delta T}{\sqrt{2}\sigma_j}\right)^2}$$

Full-rate Bang-Bang CDR

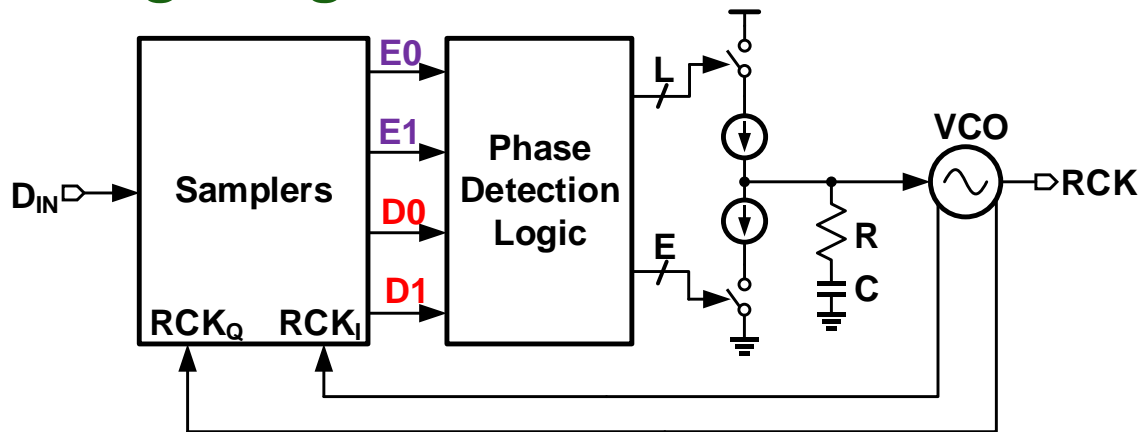


- ❑ Type-II response
- ❑ Near-zero static phase offset
- ❑ Insensitive to charge-pump non-idealities
- ❑ VCO & PD operate at full-rate or data rate ($F_{VCO} = F_{DIN}$)
 - Could become a speed bottleneck
 - Solution: Half-rate bang-bang CDR

Half-rate CDR Waveforms



Half-Rate Bang-Bang CDR



- ❑ Topology same as full-rate architecture
- ❑ Requires quadrature VCO
- ❑ Lower loop update rate → higher loop latency
- ❑ Non-linear loop dynamics due to non-linear BBPD's gain. To ensure stability^[5]

$$\text{Damping factor } \zeta = \frac{\Delta\Phi_{\text{RCK}} \text{ due to prop. path}}{\Delta\Phi_{\text{RCK}} \text{ due to integ. path}} = \frac{2RC}{T_{\text{UPDATE}}} \gg 1$$

Bang-Bang CDR Drawbacks

- ❑ Coupled JTRAN and JTOL
 - ❑ Jitter peaking
 - ❑ Large loop filter area
- } **Similar to linear CDR**
- ❑ **JGEN caused by limit cycles due to BBPD's behavior**
 - ❑ **JTRAN dependence on input jitter**

$$\text{JTRAN BW} \approx K_{PD} \cdot K_P \cdot K_{VCO}$$

$$\text{Gain } K_{PD}|_{\Delta T=0} = \frac{2V_o}{\sqrt{2\pi}\sigma_j} \implies \text{JTRAN BW} \propto \frac{1}{\sigma_j}$$

Overview

❑ Performance metrics

❑ Basic architectures

- Linear/Bang-bang
- Digital
- Hybrid

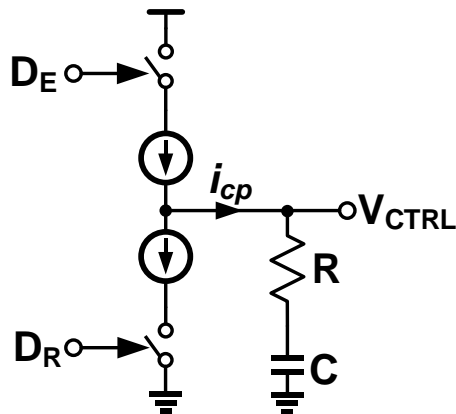
❑ Application-specific CDRs

- Multi-lane chip-to-chip links
- Repeaters for optical links and active cables

❑ Frequency detectors

Eliminating Loop Filter Capacitor

- Map CP + LF into digital domain directly

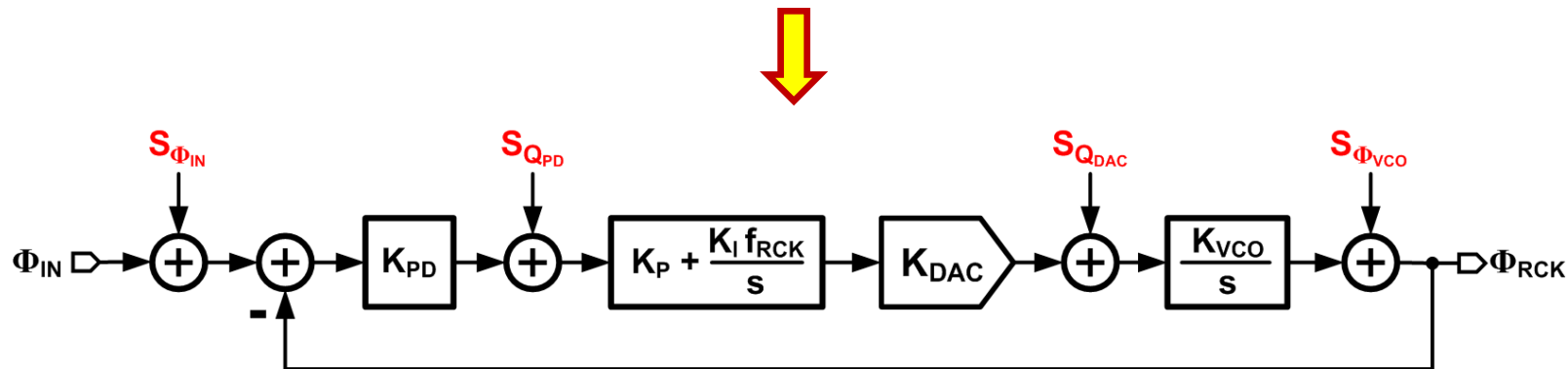
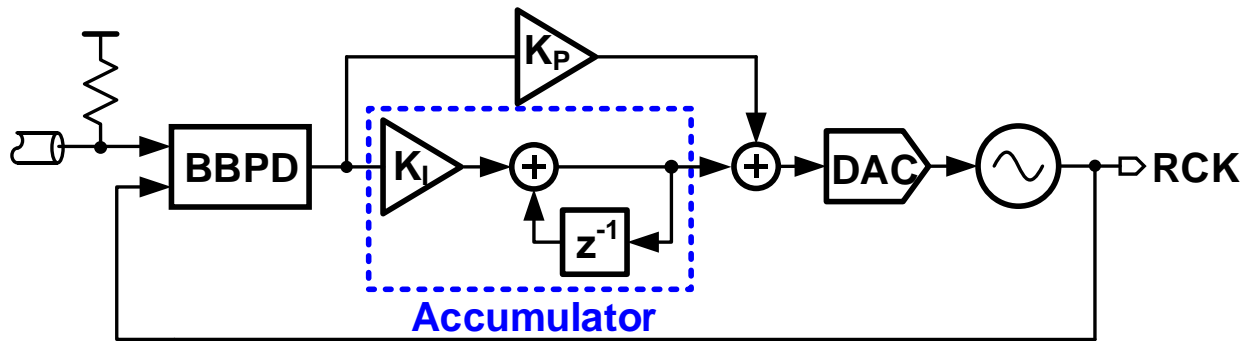


$$i_{cp}R + \frac{i_{cp}}{Cs} \Rightarrow i_{cp}R + \frac{i_{cp}T}{C} \frac{z^{-1}}{1-z^{-1}}$$

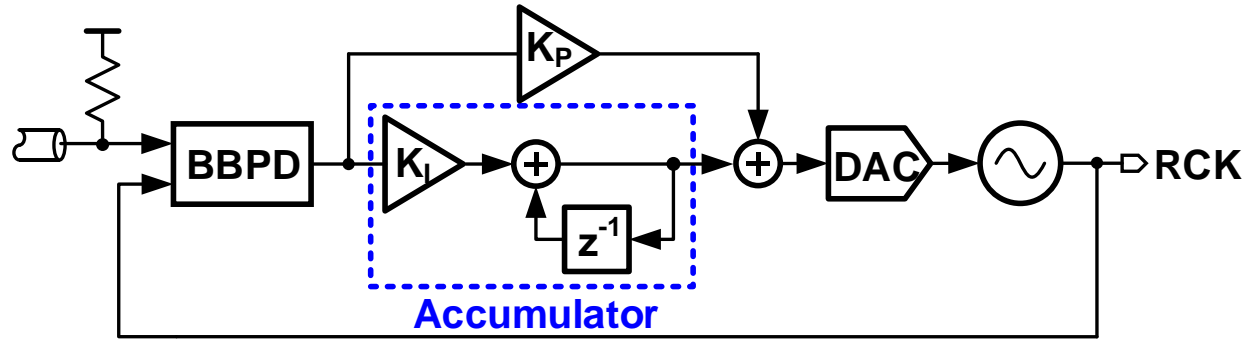
- Digital accumulator replaces loop filter capacitor

- Large time constant with small area
- Infinite DC gain \rightarrow ideal Type-II behavior
- PVT insensitive
- Easy to reconfigure for loop dynamics control

Simple Digital CDR^[6]



Simple Digital CDR^[6]

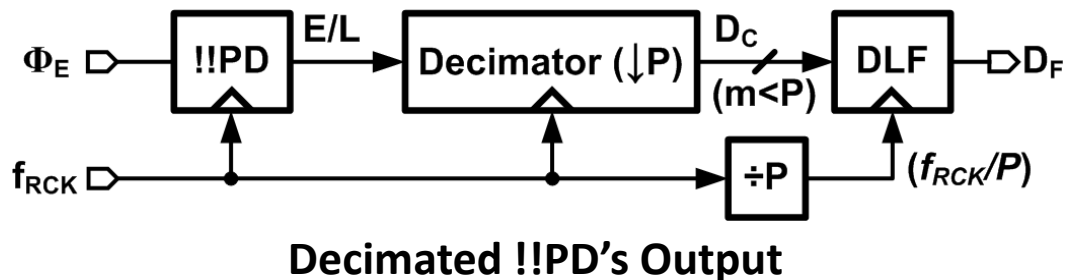
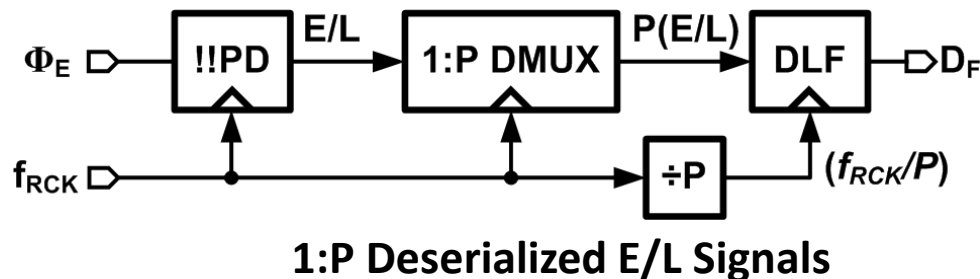
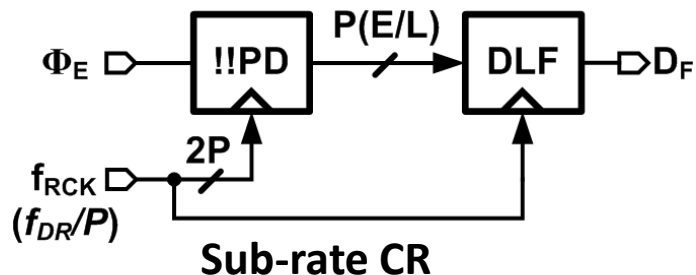


❑ Loop filter must operate at data rate

❑ Need:

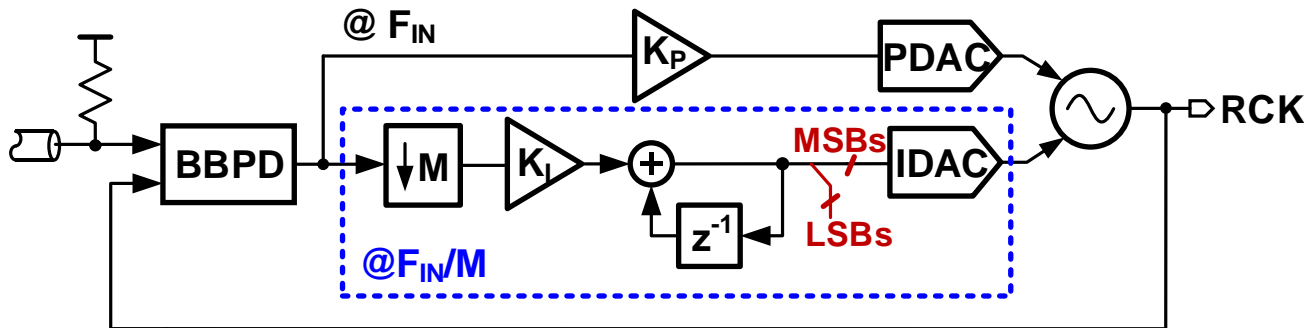
- Wide operand high-speed adders
- High speed/resolution **D**igital to **A**nalog **C**onverter (**DAC**)

Reducing Speed Requirements (I)



- ❑ DLF operates at lower speed, f_{RCK}/P . It delays feedback in the loop
- ❑ Increased loop delay adversely affects phase-margin, jitter peaking, & JTOL
- ❑ **Observation:** Proportional path dominates jitter

Reducing Speed Requirements (II)



- ❑ Fast proportional path
 - Minimize latency \rightarrow reduce dithering jitter
- ❑ High resolution integral path
 - Minimize tracking jitter
- ❑ Minimal hardware penalty
 - Needs only 2-level high-speed PDAC
- ❑ IDAC implemented using $\Delta\Sigma$ techniques
- ❑ Proportional and integral controls summed in VCO

Analog vs. Digital CDRs

❑ Analog CDR using linear PD

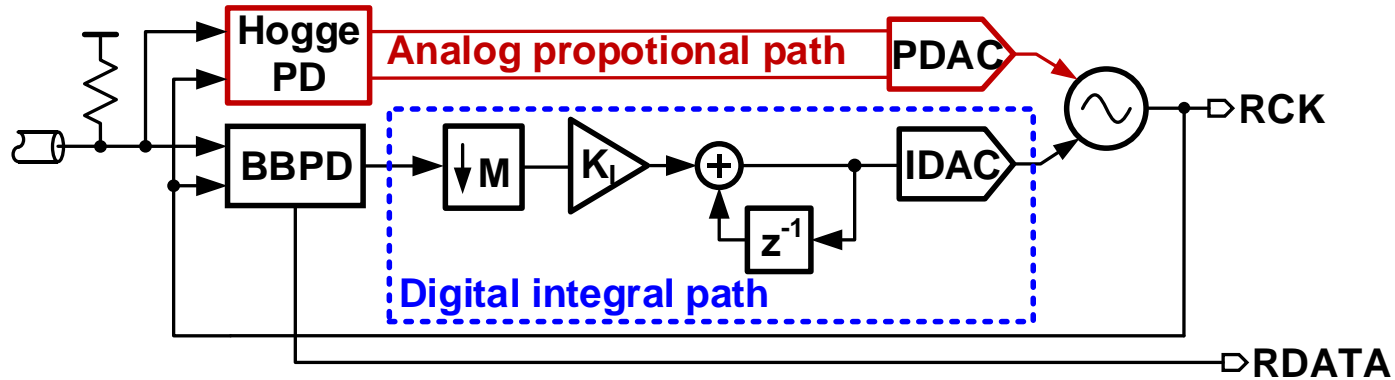
- Well-controlled loop dynamics
- PD non-idealities degrade timing margin/BER
- Large loop filter capacitor
- Sensitive to Consecutive Identical Digits (CIDs)^[7]

❑ Digital CDR using bang-bang PD

- Non-linear loop dynamics (JTRAN depends on jitter)
- Bang-bang PD maximizes timing margin
- No large capacitor (small area)
- Sensitive to Consecutive Identical Digits (CIDs)

❑ Can we combine the advantages?

Hybrid Analog/Digital CDR^[8]



□ Proportional path sets loop bandwidth (JTRAN)

- Fixed gain leads to linear loop dynamics
- Eliminates phase quantization error

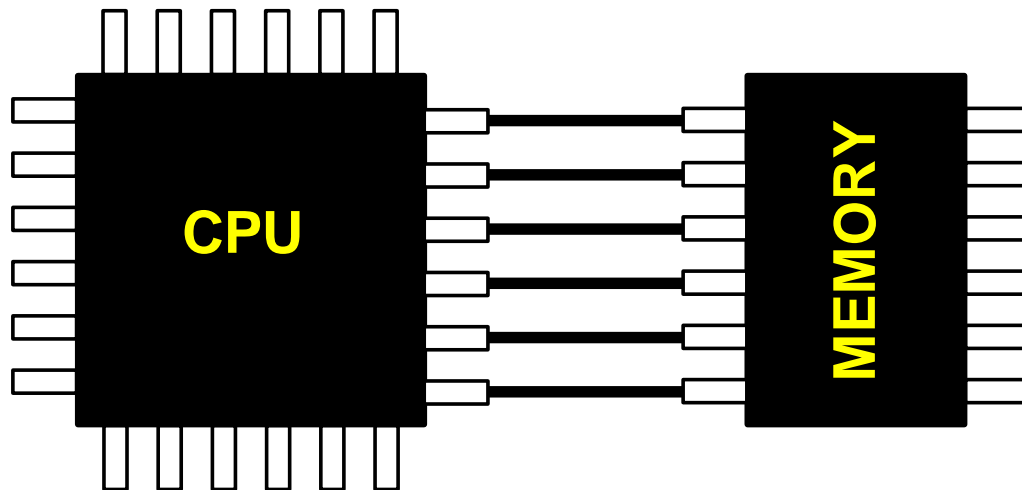
□ Digital integral path sets steady state

- Makes it insensitive to linear PD phase offset
- Accumulator filters BBPD quantization error
- BBPD's offset causes ripple on the proportional path

Overview

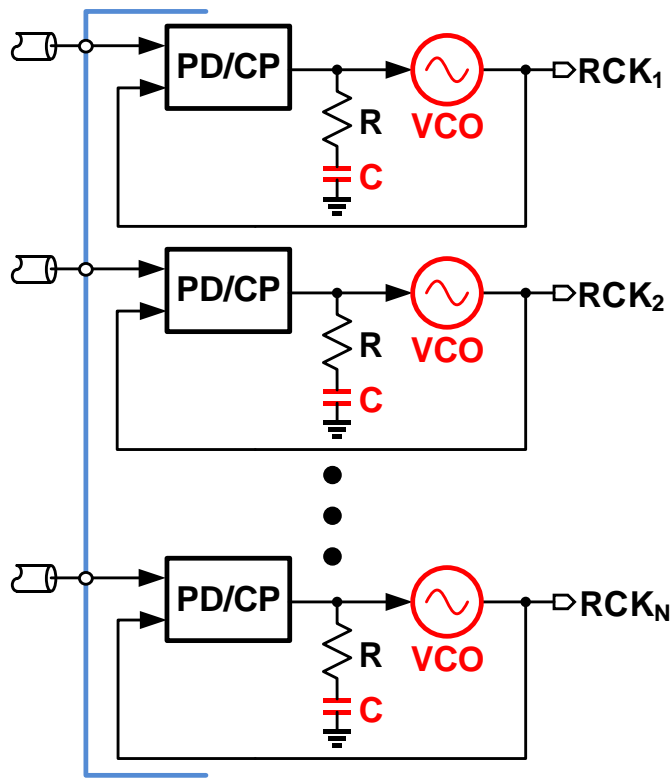
- ❑ Performance metrics
- ❑ Basic architectures
 - Linear/Bang-bang
 - Digital
 - Hybrid
- ❑ Application-specific CDRs
 - Multi-lane chip-to-chip links
 - Repeaters for optical links and active cables
- ❑ Frequency detectors

Multi-Lane Chip-to-Chip Links



- ❑ Source synchronous clocking is common
- ❑ BUT many standards mandate embedded clocking
 - Examples: PCIe, XAUI, SATA, etc.
 - Clock & data recovery is required for each lane of the multi-lane link

Multi-Lane CDR Challenges



- ❑ Many VCOs
- ❑ VCO's noise dominates low BW CDRs
- ❑ Harmonic locking
- ❑ Large capacitors & large area

Oscillators in Multi-Lane CDRs

❑ Oscillator's properties needed in multi-lane CDR

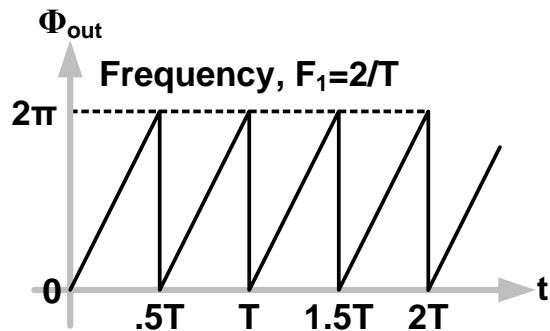
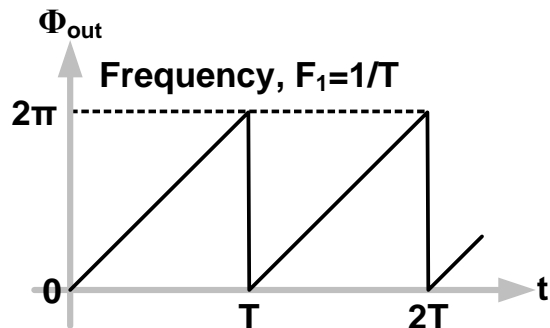
- Good phase noise performance w/ low o/p jitter
- Multiple sampling clock phases for sub-rate CDRs
- Independent & wide frequency tuning range for each lane
- Lower power consumption
- Small chip-area

	LC Oscillator	Ring Oscillator
1	Excellent phase noise	Poor phase noise
2	Low power consumption	Large power consumption compared to LC osc.
3	Limited frequency tuning range	Wide frequency tuning range
4	Reduced # of clock phases for sub-rate CDRs	Easily available clock phases for sub-rate CDRs
5	Large chip-area	Small chip-area

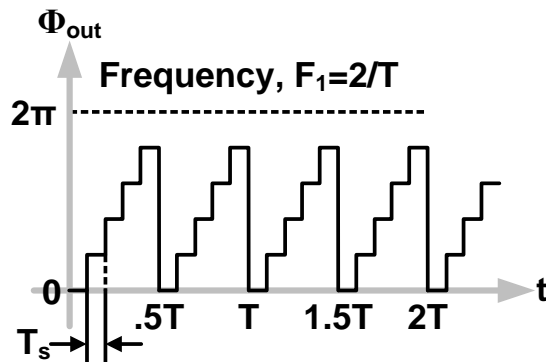
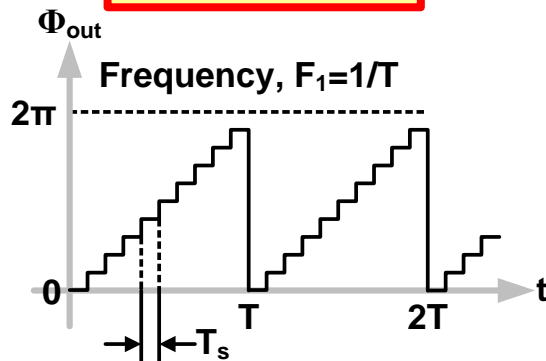
Both LC/ring-oscillators are not suited standalone for multi-lane CDRs

Phase of Analog/Digital Oscillator

Analog Oscillator



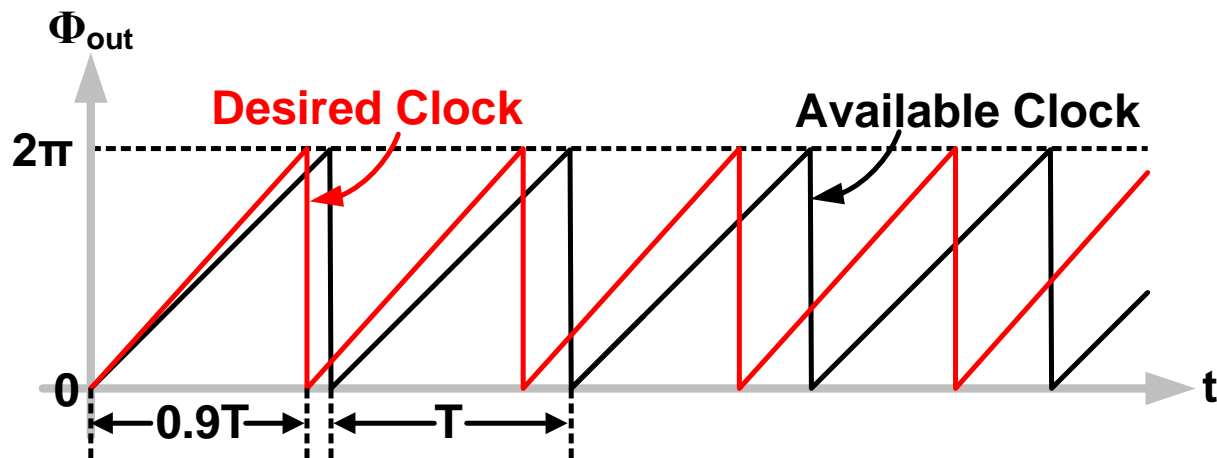
Digital Oscillator



Multiple digital clocks from

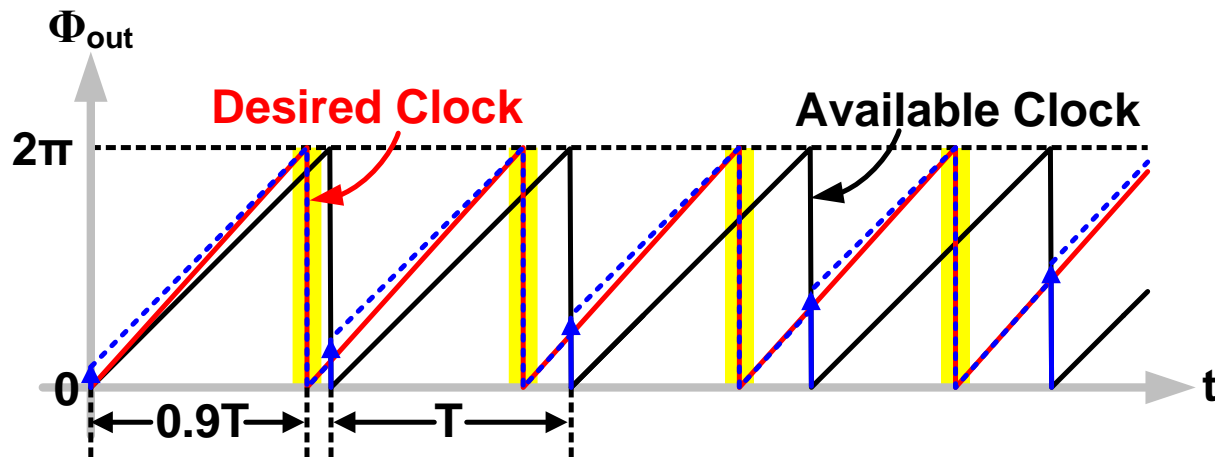
- Single clock $F_s = 1/T_s (>F_1)$
- Accumulating phase proportional to o/p frequency

Digital Oscillator Requirements in CDR



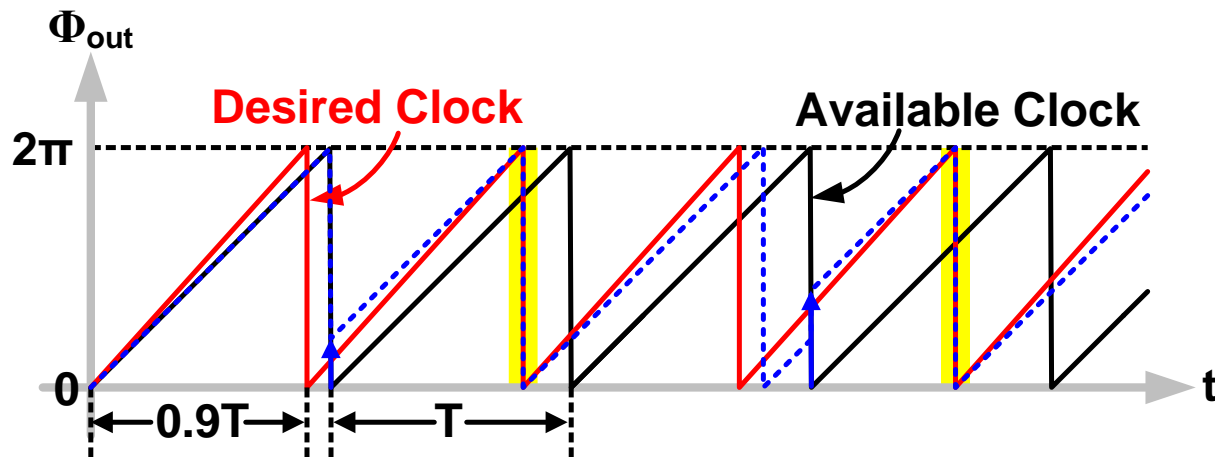
- ❑ Available clock frequency, $f_{ava}=1/T$
- ❑ Desired clock frequency, $f_{des}=1/0.9T$
- ❑ A 2π phase accumulation marks the rising or falling clock edges

Digital Oscillator w/ Desired Transitions



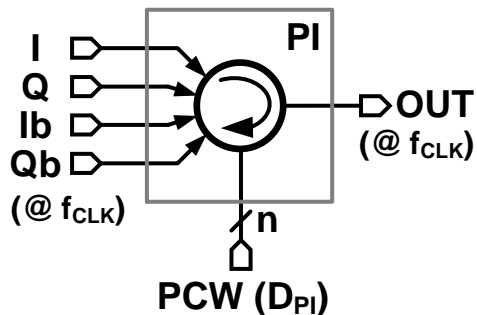
- ❑ Add accumulated phase to f_{ava} periodically
- ❑ Phase rotators, phase interpolators, etc. are used to add/subtract phase for desired frequency

Limitations of Digital Phase Addition

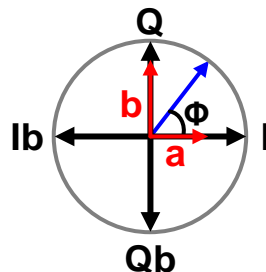


- ❑ Minimum phase addition has a lower bound
 - Leads to increased o/p jitter
 - Demands a lower CDR bandwidth
- ❑ Track desired frequency w/ reduced update rate

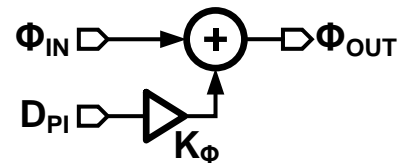
Phase Interpolator (PI)



Block Diagram



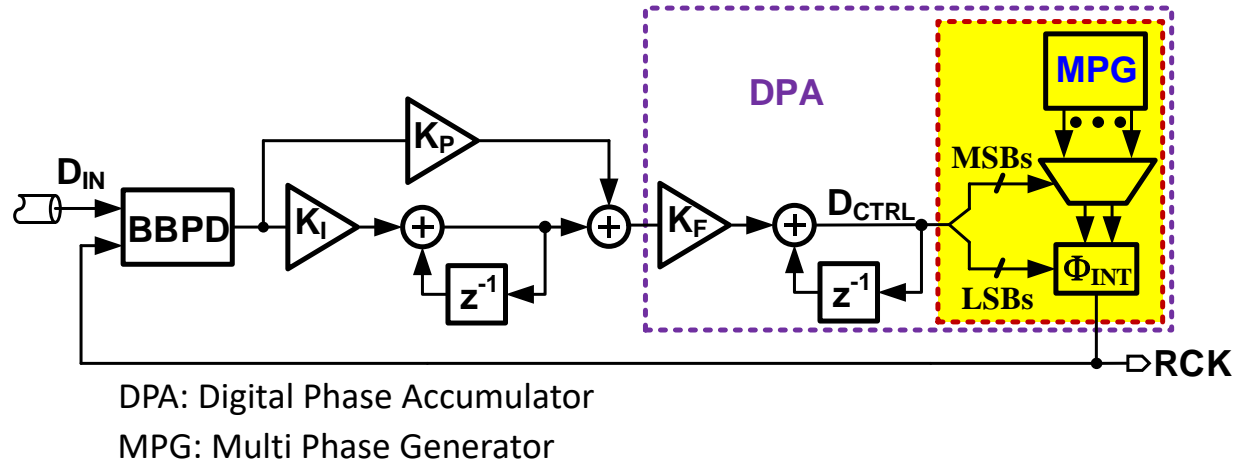
Phasor Diagram



Small Signal Model

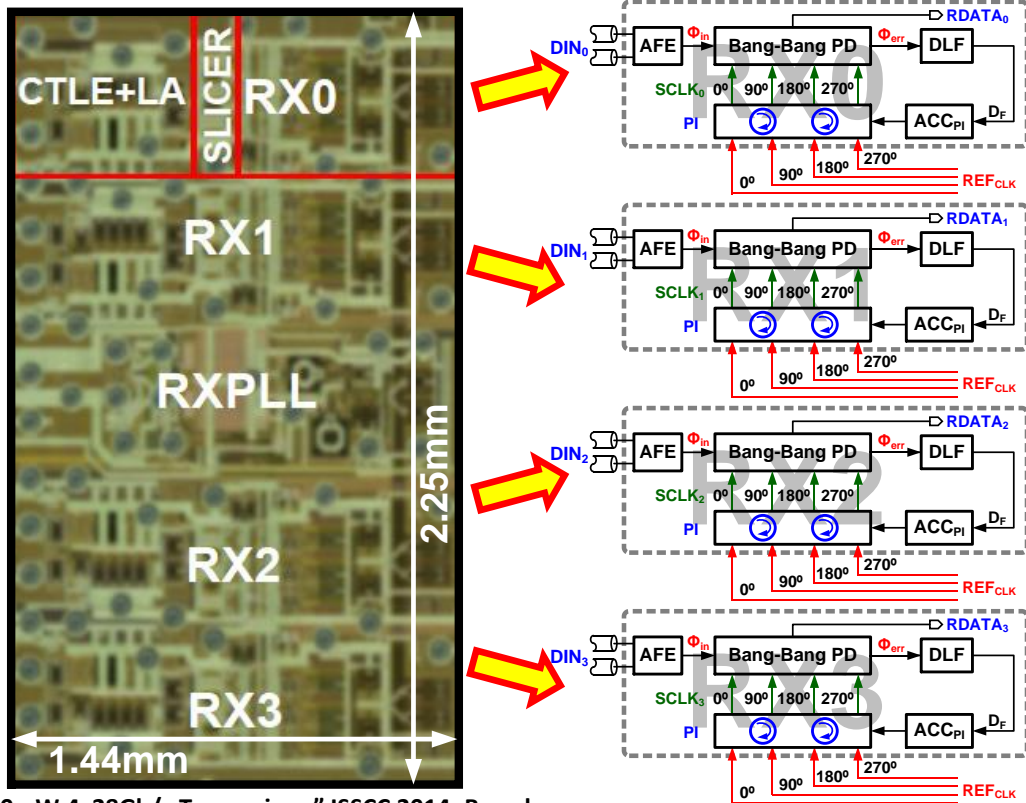
- ❑ PI interpolates I/P clock \rightarrow intermediate O/P clock
- ❑ O/P phase \propto n-bit phase control word (PCW)
- ❑ Phase resolution is limited by # of bits
- ❑ # of PIs increase with # of o/p phases required

Practical Dual-Loop CDR^[9]



- ❑ Phase interpolator (Φ_{INT}) improves DPA resolution
- ❑ Multi-phase generator is not inside CDR loop
- ❑ Accumulator + PI = Digitally Controlled Oscillator

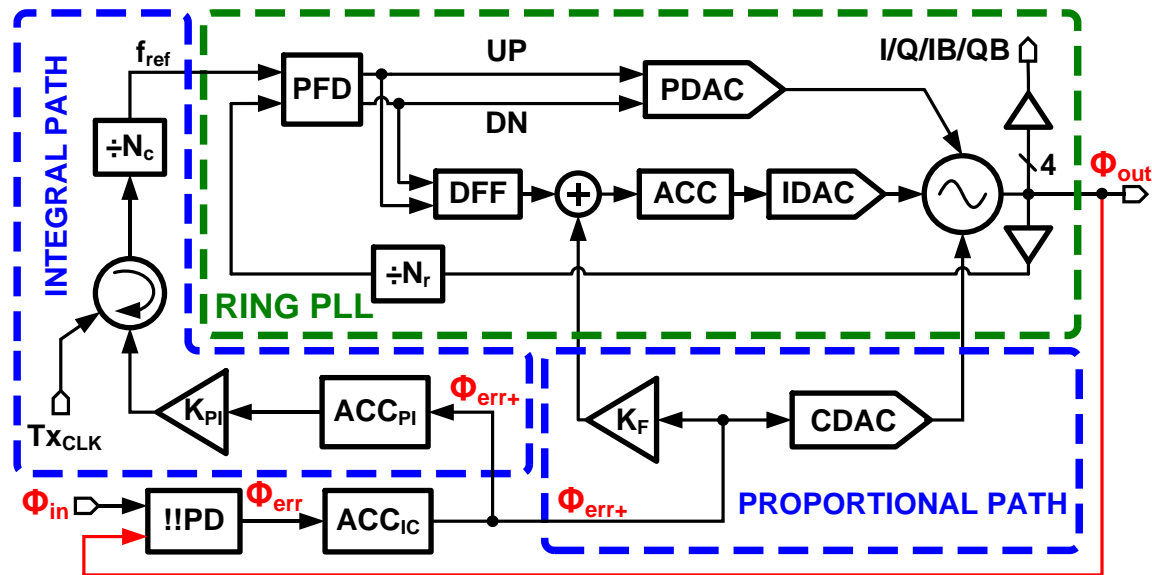
PI-based Multi-Lane Chip-to-Chip Link^[10-14]



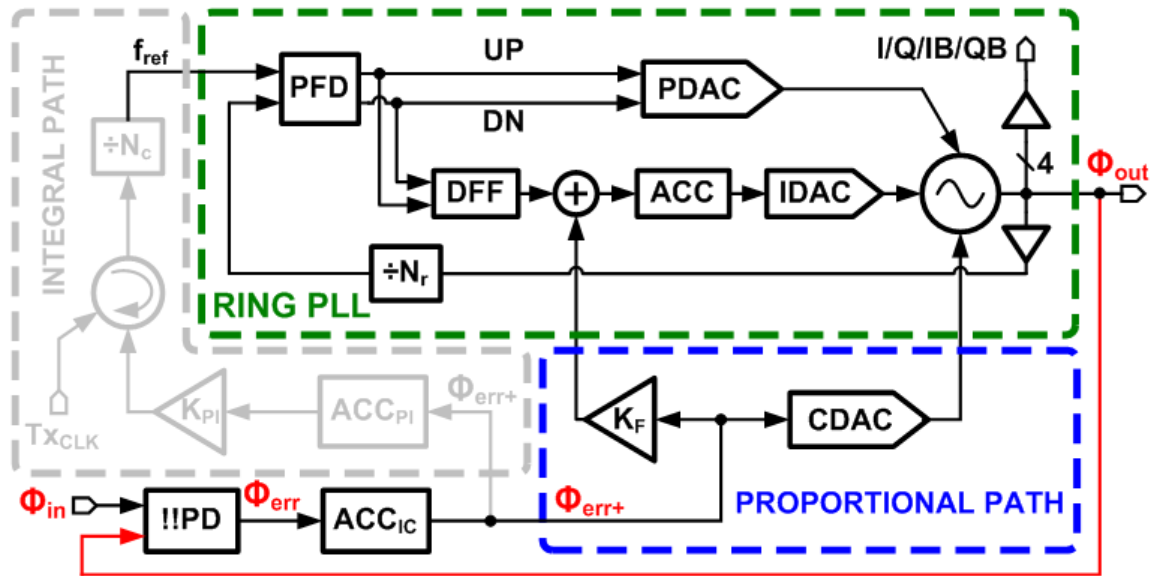
"A 780mW 4x28Gb/s Transceiver," ISSCC 2014, Broadcom

[illegible]

BBPD based Sub-rate Digital CDR w/ Embedded PLL [13]

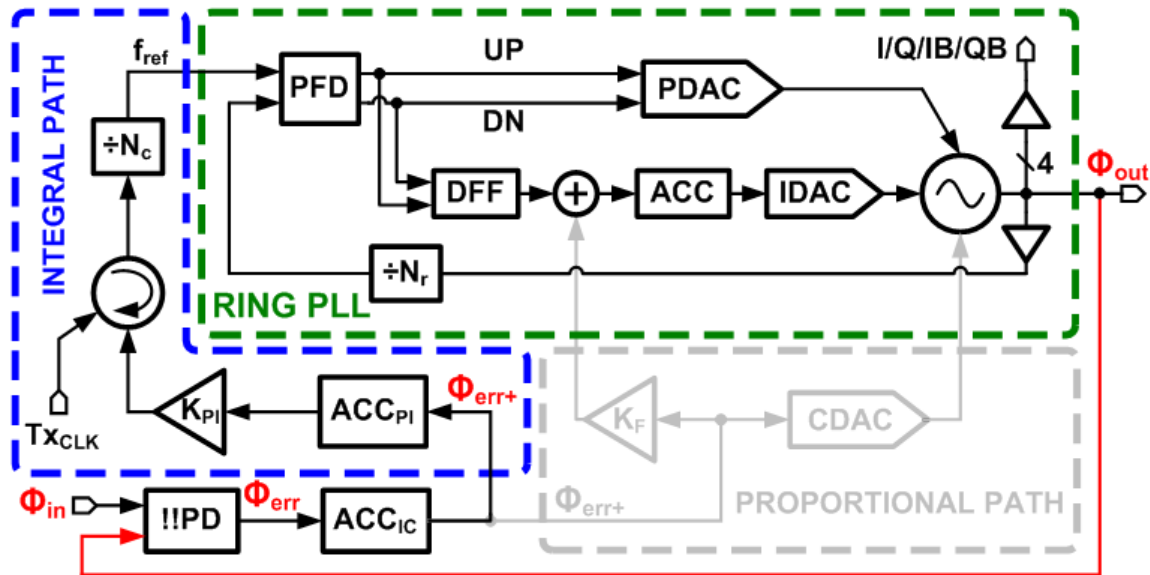


Proportional Control in Digital CDR w/ Embedded PLL (I)



$$\begin{aligned}
 LG_{prop, cdr}(s) &= \left. \frac{\Phi_{out}}{\Phi_{in}} \right|_{prop, cdr} \\
 &= \frac{K_{bbpd} f_{ref}}{s} \times \frac{N_r LG_{RPLL}(s)}{1 + LG_{RPLL}(s)} \left[\frac{K_{pc, pr} + \frac{K_{pc, ir} f_{ref}}{s}}{K_{pr} + \frac{K_{ir} f_{ref}}{s}} \right]
 \end{aligned}$$

Integral Control in Digital CDR w/ Embedded PLL (II)



$$LG_{int, cdr}(s) = \frac{K_{bbpd} K_{ic} f_{ref}^2}{s^2 N_c} \times \frac{N_r LG_{RPLL}(s)}{1 + LG_{RPLL}(s)}$$

$$\approx \frac{K_{bbpd} K_{ic} f_{ref}^2 N_r}{s^2 N_c}$$

Overview

- ❑ Performance metrics

- ❑ Basic architectures

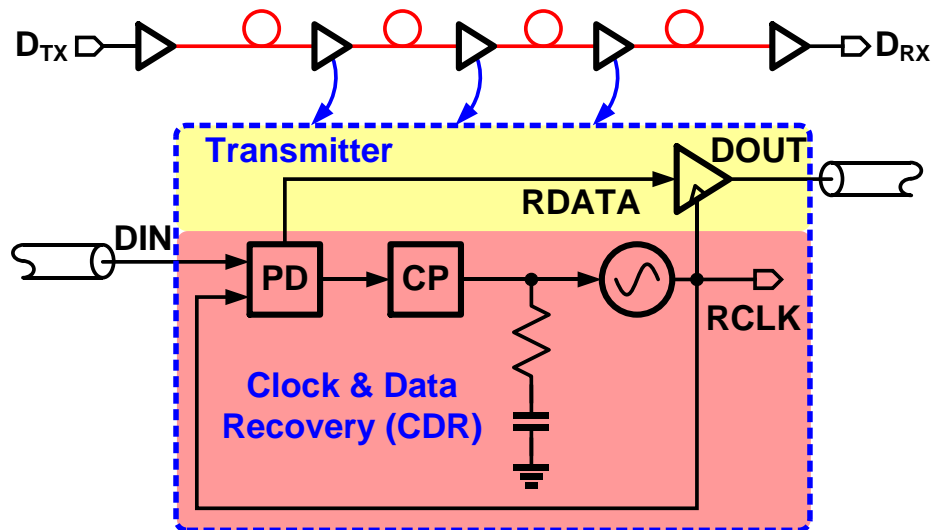
- Linear/Bang-bang
- Digital
- Hybrid

- ❑ Application-specific CDRs

- Multi-lane chip-to-chip links
- Repeaters for optical links and active cables

- ❑ Frequency detectors

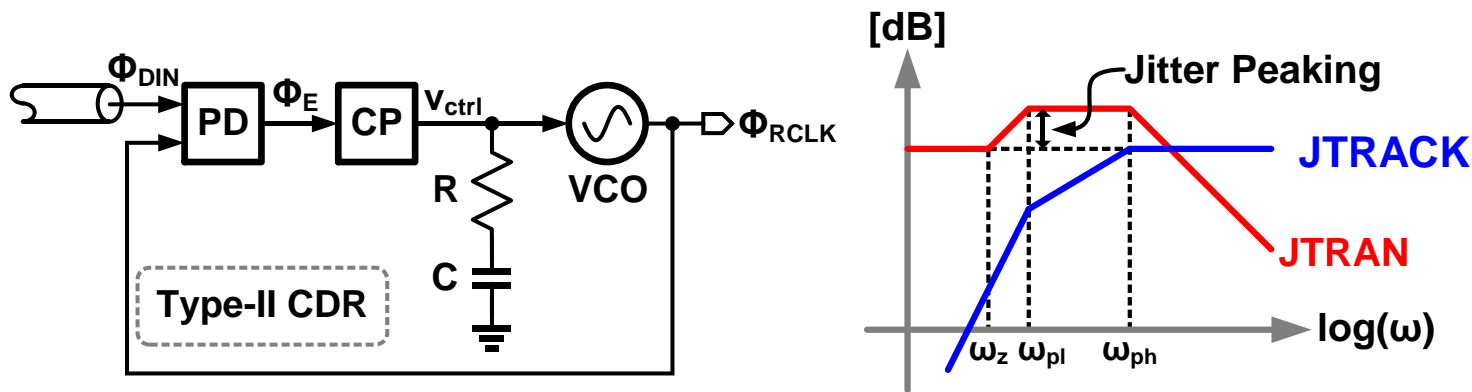
Long Haul Communication w/ Repeaters



□ Repeater requirements

- Tolerate large input jitter present on DIN (high JTOL)
- Filter input jitter (low JTRAN BW) w/ minimal peaking
- Re-transmit with low jitter (low JGEN)

Conventional Type-II CDR in Repeaters

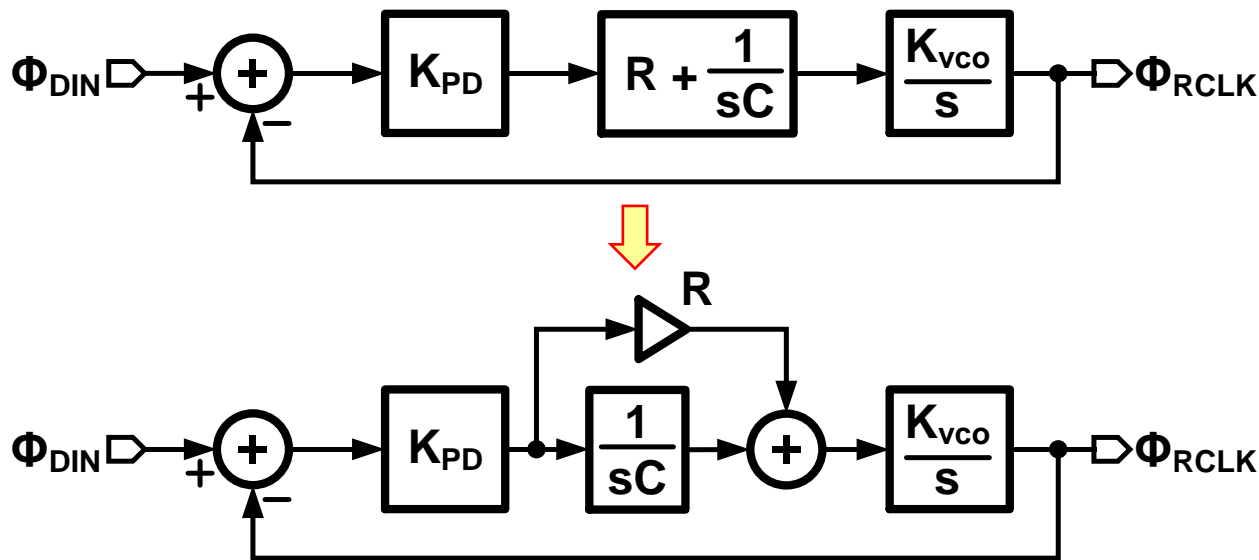


- ❑ ω_z is cause for jitter peaking in forward path but must for stability
- ❑ High JTRACK BW (or JTOL corner freq.) \rightarrow high JTRAN BW
- ❑ Inadequate filtering of $\Phi_{DIN} \rightarrow$ more R_{CLK} jitter \rightarrow Retransmission with more jitter

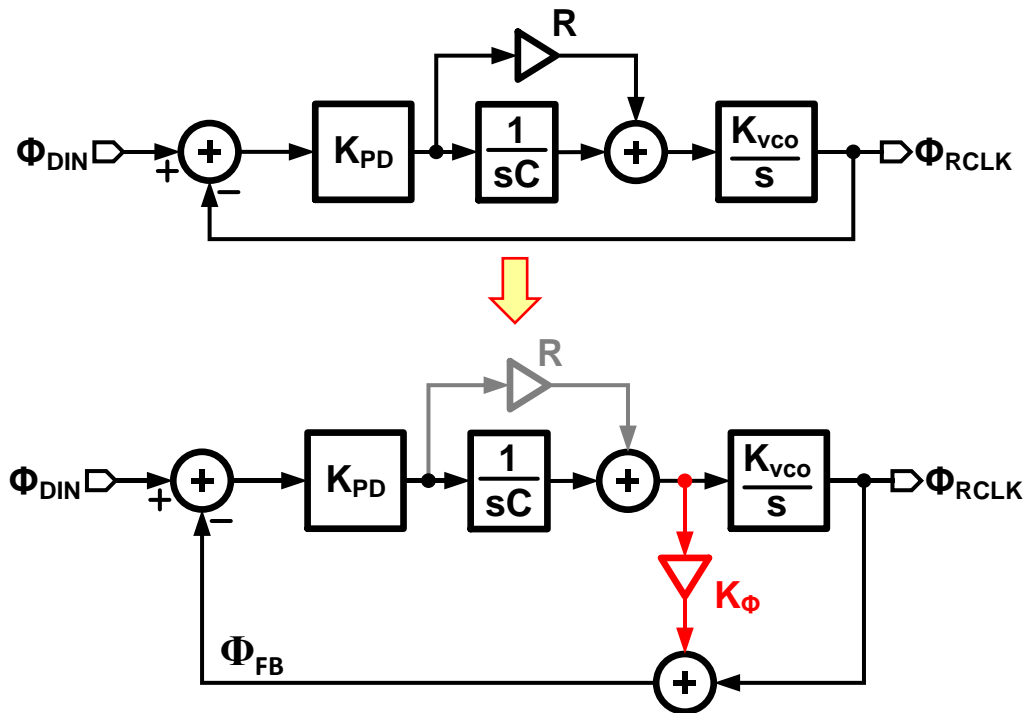
How to Eliminate Jitter Peaking?

□ Main Idea:

- Retain ω_z in loop for stability
- Remove ω_z from forward path to eliminate peaking

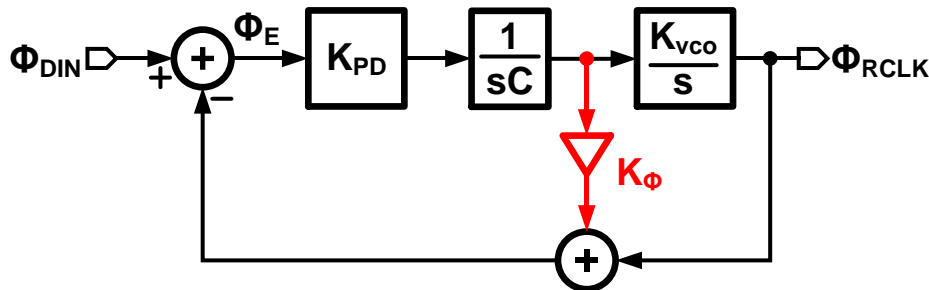


Add to VCO's Output Phase (I)



❑ No zero in feed-forward path

Add to VCO's Output Phase (II)



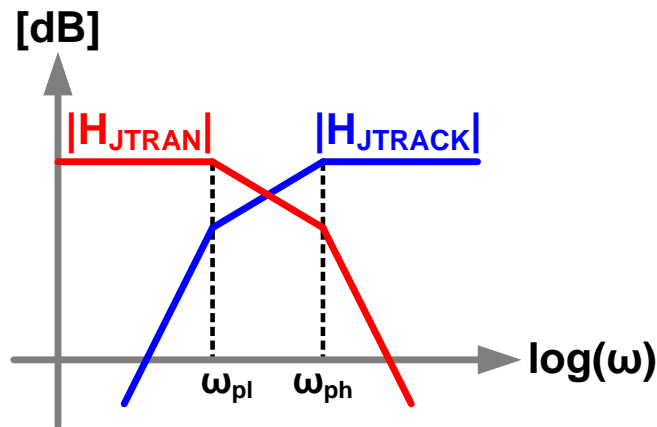
$$LG(s) = \frac{K_{PD}K_{VCO}}{s^2C} \left(1 + \frac{sK_\phi}{K_{VCO}} \right) = \frac{K}{s^2} (1 + s/\omega_z)$$

$$H_{JTRAN} = \frac{\Phi_{RCLK}(s)}{\Phi_{DIN}(s)} = \frac{LG(s)}{1 + LG(s)} \frac{1}{(1 + s/\omega_z)} = \frac{K_{PD}K_{VCO}}{s^2C + sK_{PD}K_\phi + K_{PD}K_{VCO}}$$

$$H_{JTRACK} = \frac{\Phi_E(s)}{\Phi_{DIN}(s)} = \frac{1}{1 + LG(s)} = \frac{s^2}{s^2C + sK_{PD}K_\phi + K_{PD}K_{VCO}}$$

- ❑ Phase is added to output clock, RCLK
- ❑ Loop can be stable with no jitter peaking ($\zeta > 0.707$)

Decoupled JTRAN & JTRACK/JTOL

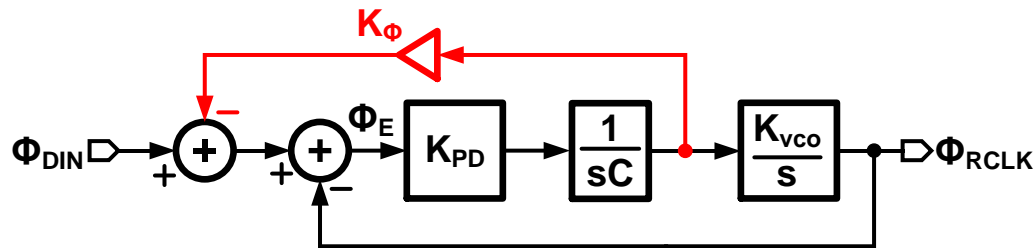


$$H_{JTRAN}(s) = \frac{\Phi_{RCLK}(s)}{\Phi_{DIN}(s)} = \frac{K_{PD}K_{vco}}{s^2C + sK_{PD}K_{\phi} + K_{PD}K_{vco}}$$

$$H_{JTRACK}(s) = \frac{\Phi_E(s)}{\Phi_{DIN}(s)} = \frac{s^2}{s^2C + sK_{PD}K_{\phi} + K_{PD}K_{vco}}$$

- $\omega_{pl} (\approx K_{PD}K_{\phi}/C)$ limits JTRAN bandwidth
- $\omega_{ph} (\approx K_{VCO}/K_{\phi})$ limits JTRACK or JTOL bandwidth

Add to Input Phase (II)^[15]



$$LG(s) = \frac{K_{PD}K_{vco}}{s^2C} \left(1 + \frac{sK_{\phi}}{K_{vco}} \right) = \frac{K}{s^2} (1 + s/\omega_z)$$

$$H_{JTRAN}(s) = \frac{\Phi_{RCLK}(s)}{\Phi_{DIN}(s)} = \frac{LG(s)}{1 + LG(s)} \frac{1}{(1 + s/\omega_z)} = \frac{K_{PD}K_{vco}}{s^2C + sK_{PD}K_{\phi} + K_{PD}K_{vco}}$$

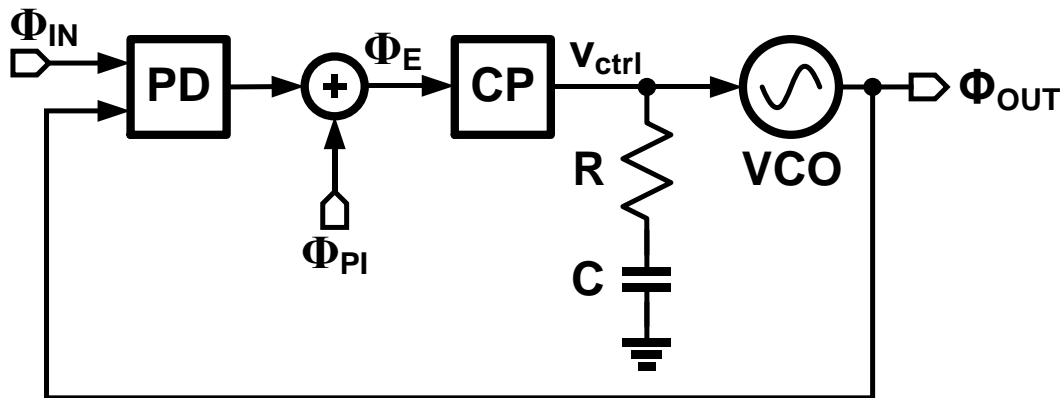
$$H_{JTRACK}(s) = \frac{\Phi_E(s)}{\Phi_{DIN}(s)} = \frac{1}{1 + LG(s)} = \frac{s^2}{s^2C + sK_{PD}K_{\phi} + K_{PD}K_{vco}}$$

- ❑ Phase is added to input data, DIN
- ❑ JTRAN and JTOL/JTRACK are decoupled

How to Add Phase to Input/Output ?

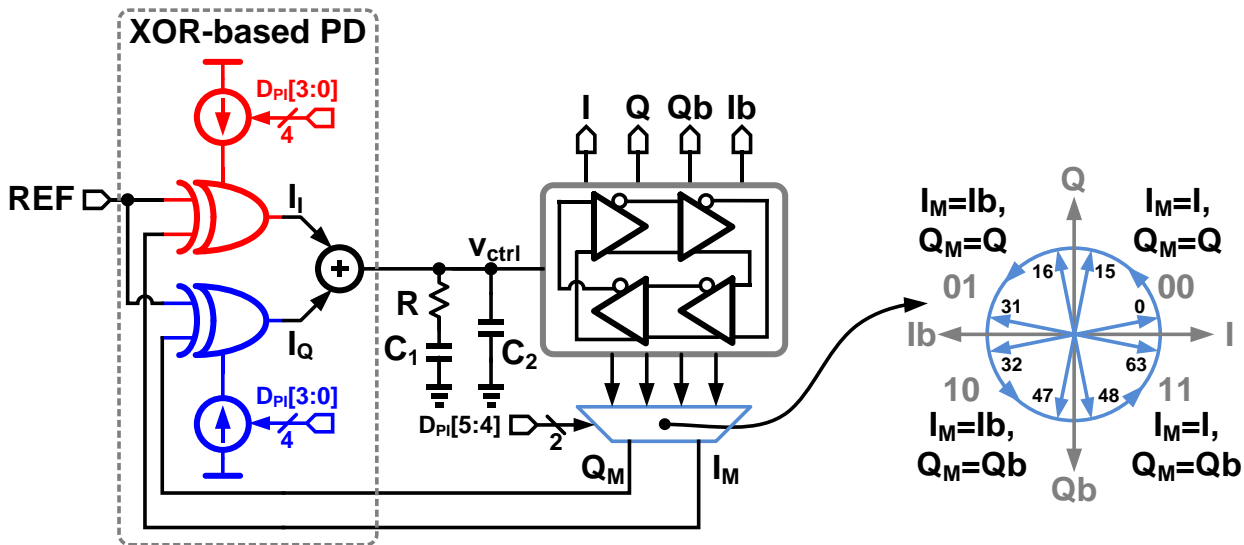
- ❑ Phase Interpolator (PI)
- ❑ Phase Rotating Phase-Locked Loop (PRPLL)
- ❑ Delay Line

PRPLL's Basic Principle



- ❑ Φ_{PI} is an external phase added to PLL
- ❑ In steady state of PLL, $\Phi_{OUT} = \Phi_{IN} - \Phi_{PI}$
- ❑ Ring oscillator (VCO) generates multiple output clock phases shifted by Φ_{PI} and used in CDR

Phase-Rotating Phase-Locked Loop



- ❑ PLL generates multiple clock phases ($I/Q/Ib/Qb$)
- ❑ Phase added to output clock in XOR-PD through D_{PI}
- ❑ $D_{PI}[5:4]$ select I_M & Q_M from clock phases I, Q, Ib, Qb
- ❑ $D_{PI}[3:0]$ change weight of I_M & Q_M in XOR-PD

How to Add Phase to Input/Output ?

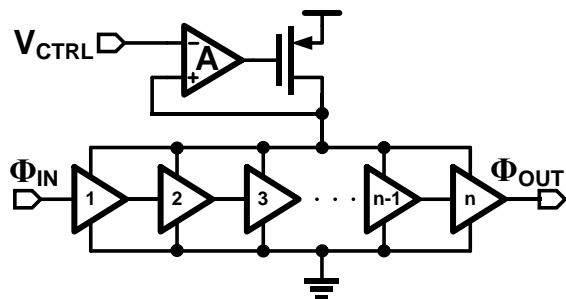
☐ Phase Interpolator (PI)

☐ Phase Rotating Phase-Locked Loop (PRPLL)

☒ Delay Line

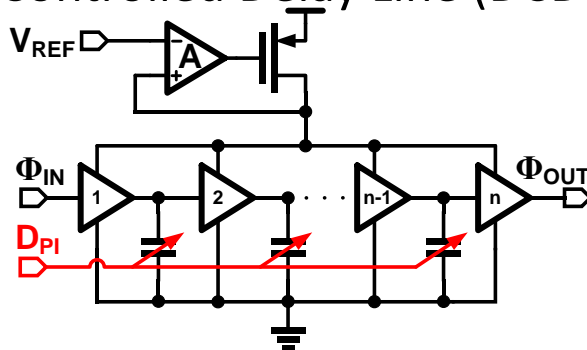
Delay Line

□ Voltage Controlled Delay Line (VCDL)



$$\Phi_{OUT} = \Phi_{IN} + K_{VCDL} \cdot V_{CTRL}$$

□ Digitally Controlled Delay Line (DCDL)



$$\Phi_{OUT} = \Phi_{IN} + K_{DCDL} \cdot D_{PI}$$

Comparison b/w Phase Addition Methods

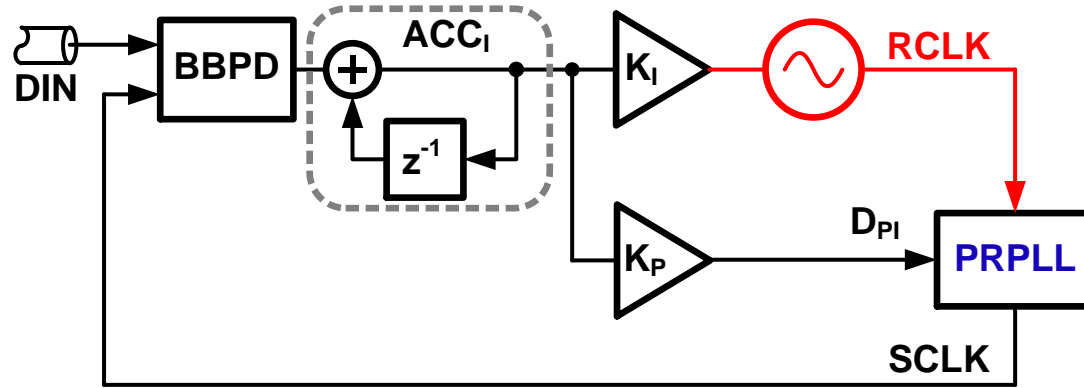
	PI	PRPLL	Delay Line
Architecture	Open loop	Closed loop	Open loop
Range	Infinite	Infinite	Limited
Φ added to CLK	Yes	Yes	Yes
Φ added to Data	No	No	Yes
Hardware for sub-rate CDRs	Increases	No change	Increases for CLK, No change for Data

- ❑ Φ addition in data path adds to data dependent ISI

CDR Examples w/ JTRAN & JTOL Decoupling

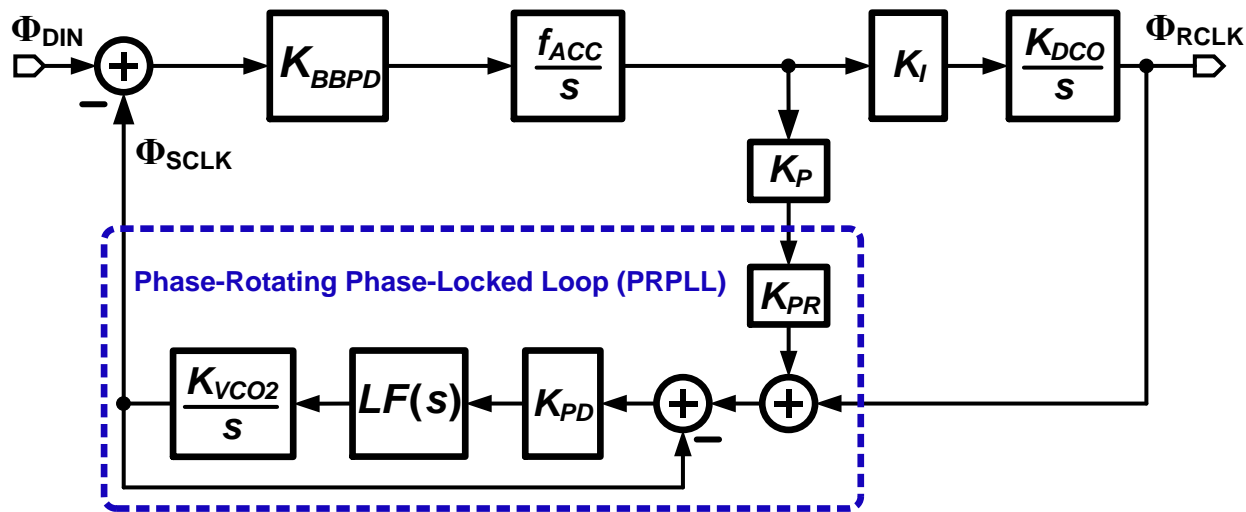
- ❑ Digital clock & data recovery using phase-rotating phase-locked loop (PRPLL)
- ❑ Digital clock & data recovery using digitally controlled delay line in data path

Block Diagram of 5Gb/s PRPLL-based Digital CDR^[21]



- ❑ Input jitter is filtered at recovered clock O/P, RCLK
- ❑ Input jitter is tracked at sampling clock, SCLK, using phase-rotating phase-locked loop (PRPLL)
- ❑ Recovered clock is a reference for PRPLL

Linearized Model of PRPLL-based Digital CDR



$$LG(s) = \rho K_{BBPD} \frac{f_{ACC}}{s} \left(K_P K_{PR} + \frac{K_I K_{DCO}}{s} \right) \times \frac{LG_{PRPLL}(s)}{1 + LG_{PRPLL}(s)}$$

$$LG_{PRPLL}(s) = K_{PD} LF(s) \frac{K_{VCO2}}{s}$$

□ ρ is input transition density

Loop Analysis of PRPLL-based Digital CDR

Approximating, $\frac{L_{GPRPLL}(s)}{1 + L_{GPRPLL}(s)} \approx 1$

$$H_{IN2RCLK} = \frac{\Phi_{RCLK}(s)}{\Phi_{DIN}(s)} = \frac{\rho K_{BBPD} f_{ACC} K_I K_{DCO}}{s^2 + s \rho K_{BBPD} f_{ACC} K_P K_{PR} + \rho K_{BBPD} f_{ACC} K_I K_{DCO}}$$

$$H_{IN2SCLK} = \frac{\Phi_{SCLK}(s)}{\Phi_{DIN}(s)} = \frac{s \rho K_{BBPD} f_{ACC} K_P K_{PR} + \rho K_{BBPD} f_{ACC} K_I K_{DCO}}{s^2 + s \rho K_{BBPD} f_{ACC} K_P K_{PR} + \rho K_{BBPD} f_{ACC} K_I K_{DCO}}$$

$$\omega_{p1} = \frac{K_{PP}}{2} \left(1 - \sqrt{1 - \frac{4K_{INT}}{K_{PP}^2}} \right) \approx \frac{K_{INT}}{K_{PP}} = \frac{K_I K_{DCO}}{K_P K_{PR}}$$

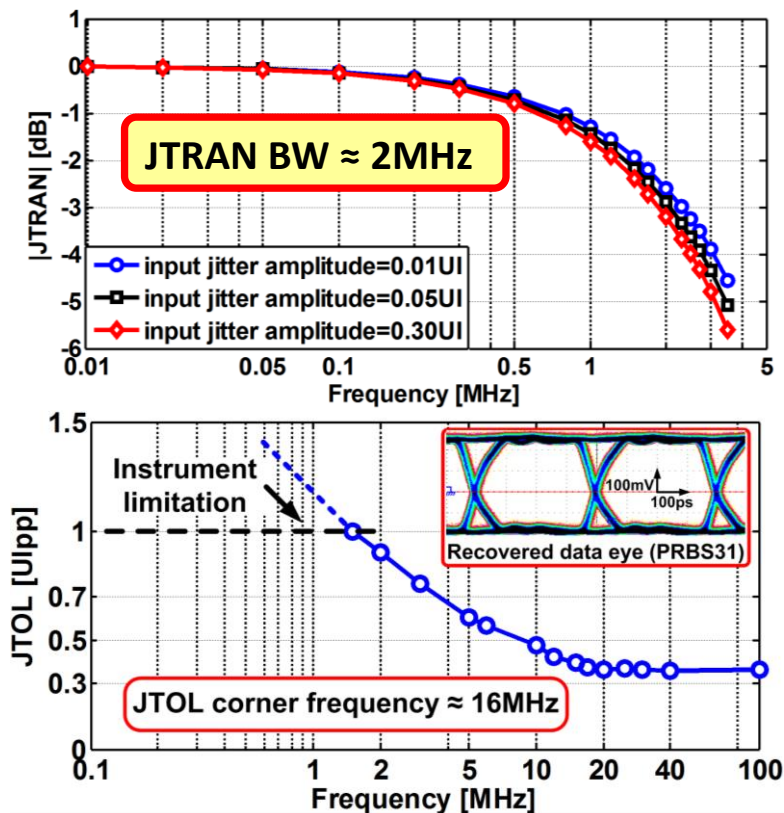
$$\omega_{p2} = \frac{K_{PP}}{2} \left(1 + \sqrt{1 - \frac{4K_{INT}}{K_{PP}^2}} \right) \approx K_{PP} = \rho K_{BBPD} f_{ACC} K_P K_{PR}$$

□ No peaking for $Q_P = \frac{\sqrt{K_{INT}}}{K_{PP}} \leq \frac{1}{\sqrt{2}}$

□ In general, ω_{p1} limits JTRAN bandwidth and ω_{p2} limits JTRACK bandwidth

PRPLL-based Digital CDR Measurement Results (I)

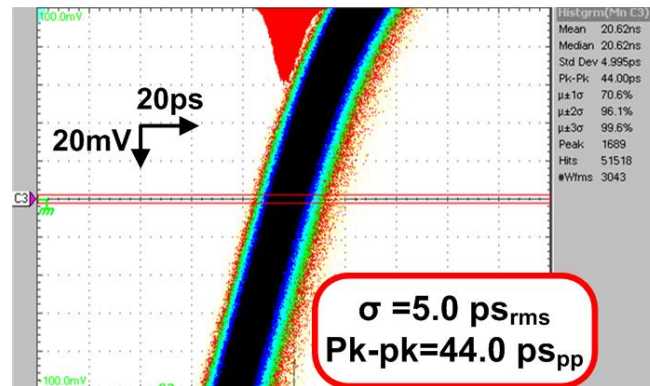
K_{PR}	$2\pi/64$ rad/s
K_{DCO}	$2\pi \times 10^5$ rad/s/LSB
K_p	0.5
K_I	0.25
f_{ACC}	$f_{VCO}/4$
DCO's PN	-100 dBc/Hz @1M
DCO's DAC	0.4 MHz/LSB



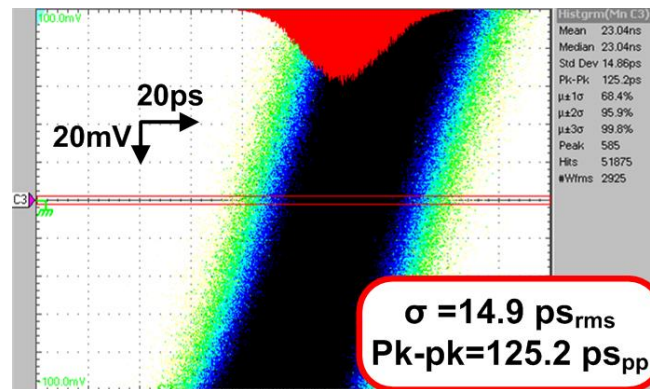
PRPLL-based Digital CDR Measurement Results (II)

K_{PR}	$2\pi/64 \text{ rad/s}$
K_{DCO}	$2\pi \times 10^5 \text{ rad/s/LSB}$
K_p	0.5
K_I	0.25
f_{ACC}	$f_{VCO}/4$
DCO's PN	-100 dBc/Hz @1M
DCO's DAC	0.4 MHz/LSB

Recovered Clock



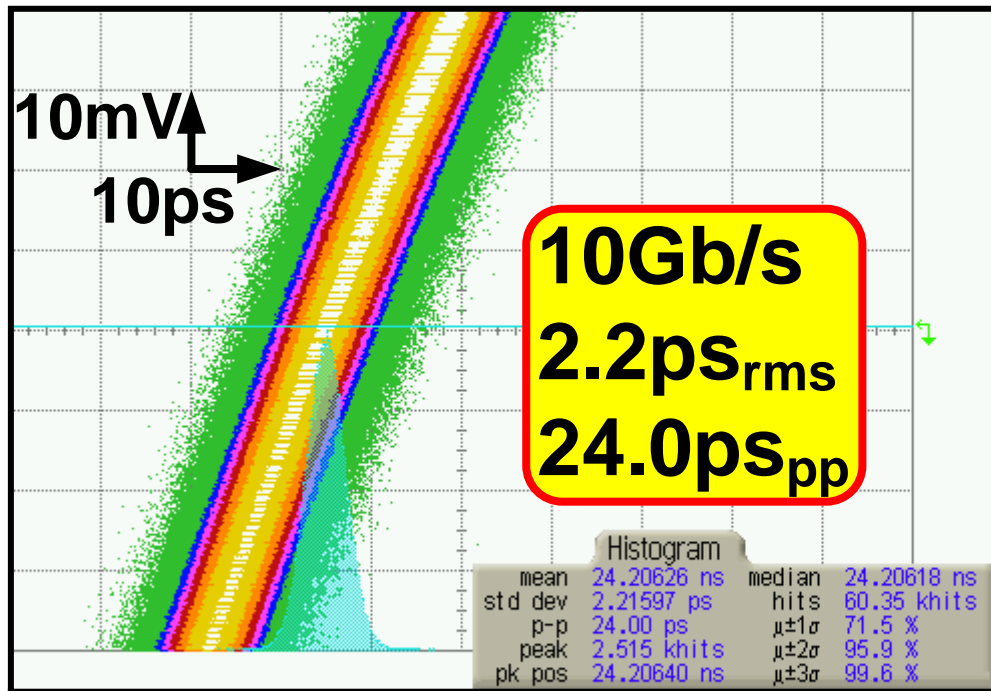
Sampling Clock



CDR Examples w/ JTRAN & JTOL Decoupling

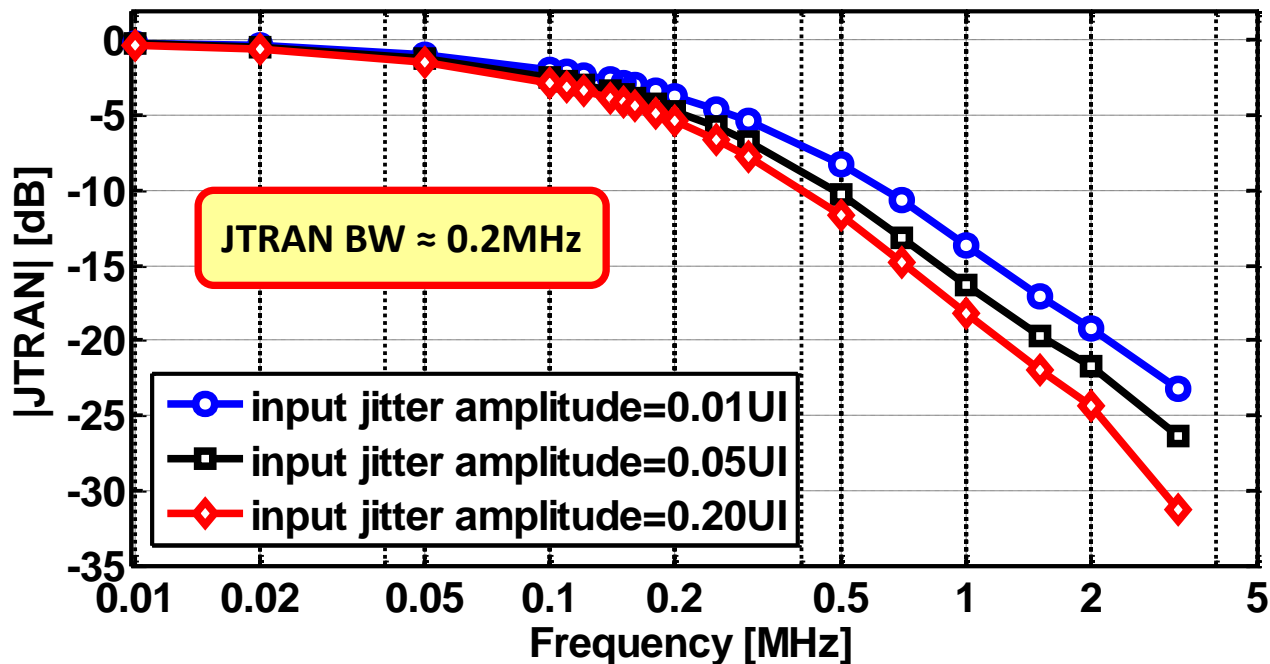
- ❑ Digital clock & data recovery using phase-rotating phase-locked loop (PRPLL)
- ❑ Digital clock & data recovery using digitally controlled delay line in data path

Recovered Clock of CDR locked at 10Gb/s



□ 2.2 ps_{rms} jitter for 5GHz recovered clock (R_{CLK})

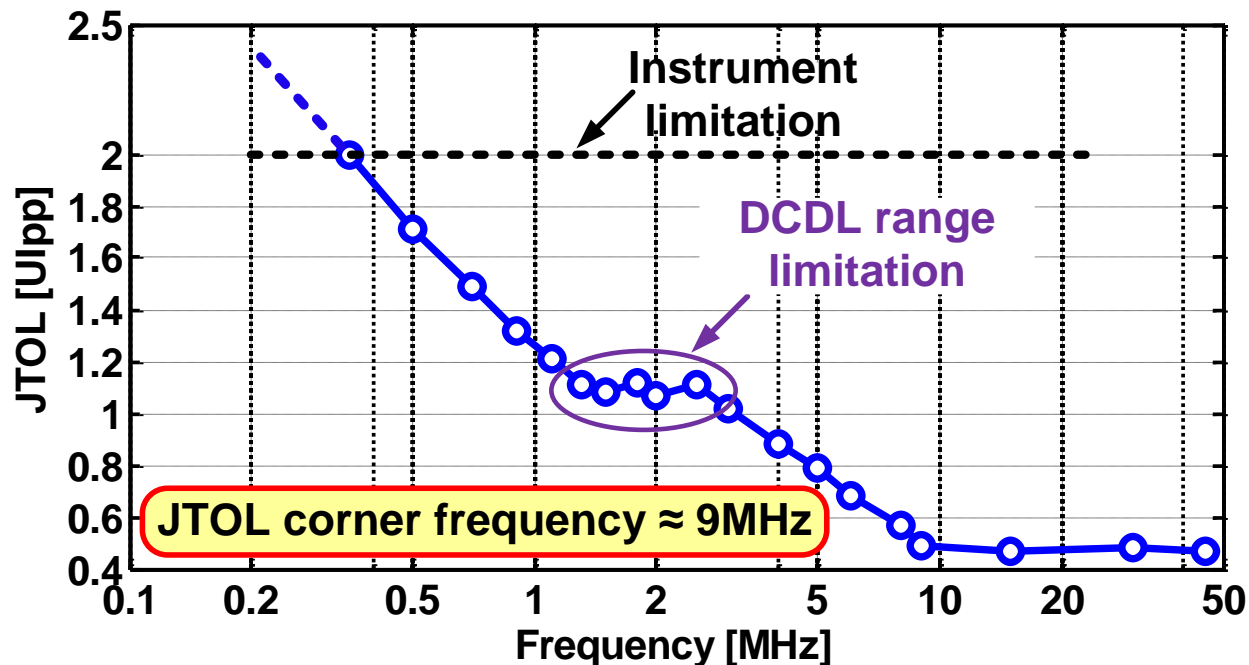
Measured Jitter Transfer Function (JTRAN)



□ CDR is locked to 10Gb/s input data

□ JTRAN bandwidth ≈ 0.2 MHz

Measured Jitter Tolerance (JTOL)

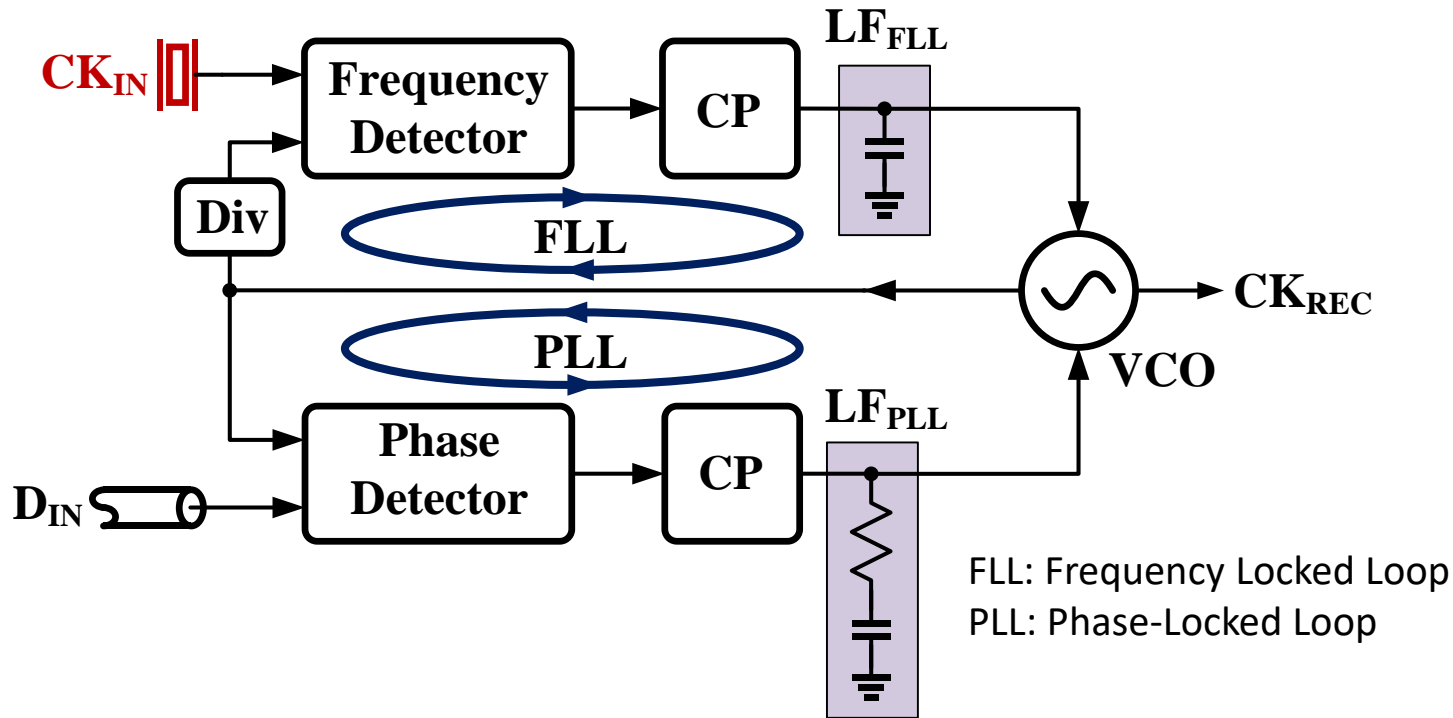


□ JTOL measured w/ BER threshold of 10^{-12} & PRBS7 data 10Gb/s

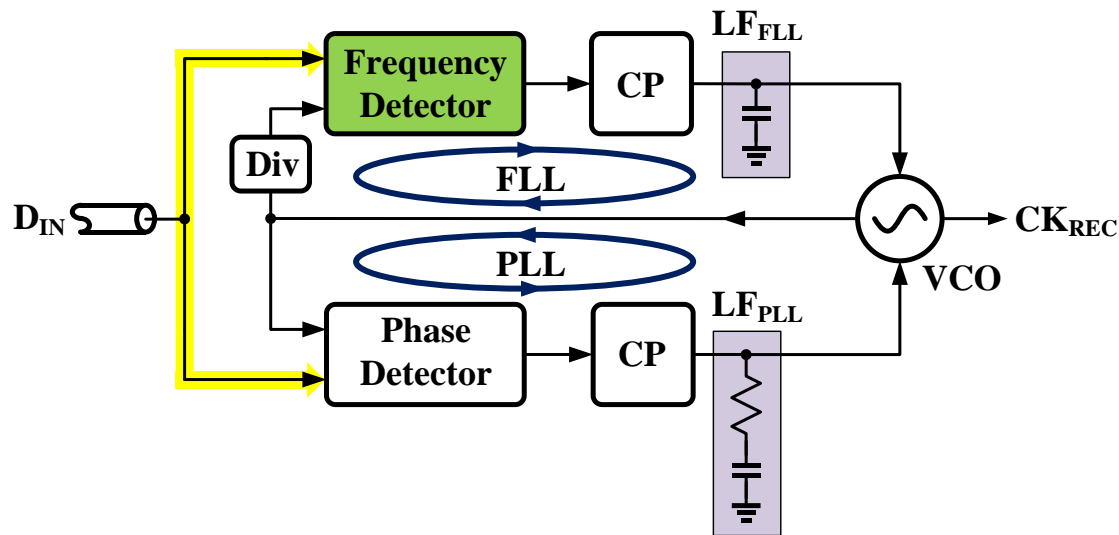
Overview

- ❑ Performance metrics
- ❑ Basic architectures
 - Linear/Bang-bang
 - Digital
 - Hybrid
- ❑ Application-specific CDRs
 - Multi-lane chip-to-chip links
 - Repeaters for optical links and active cables
- ❑ Frequency detectors

Frequency & Phase Tracking in CDRs

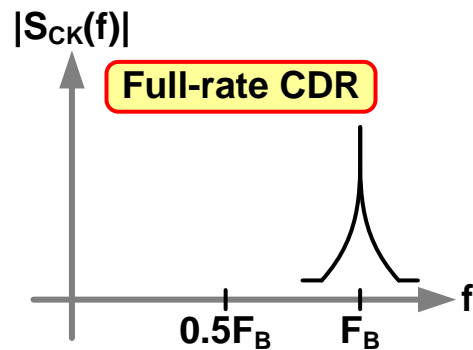
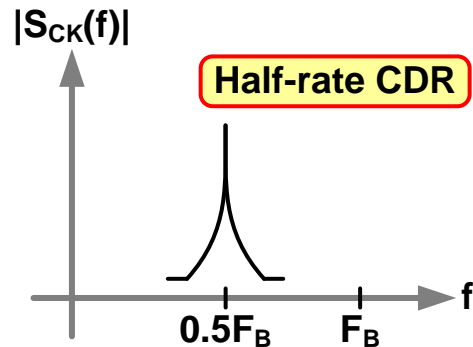
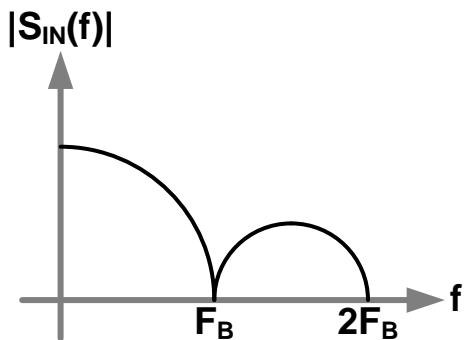


Reference-less CDR



- ❑ Reference extracted from incoming random data
- ❑ Continuous data-rate
- ❑ Requires *frequency extraction* from random data

Role of FLL: Frequency Domain View



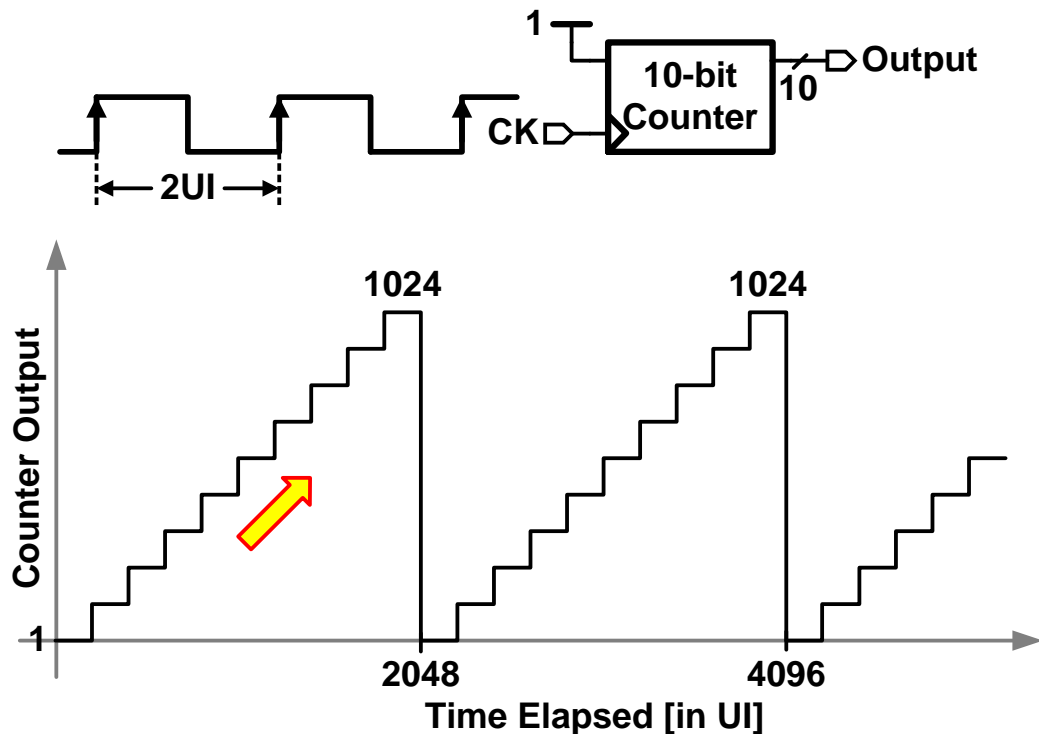
Frequency Detector

- ❑ Rotational frequency detector^[22-24]
- ❑ Quadri-correlator frequency detector^[25-26]
- ❑ Stochastic reference clock generator^[27]
- ❑ Miscellaneous FDs
 - Strobed linear PD^[27]
 - Counting based FDs^[28-29]

Frequency Detector

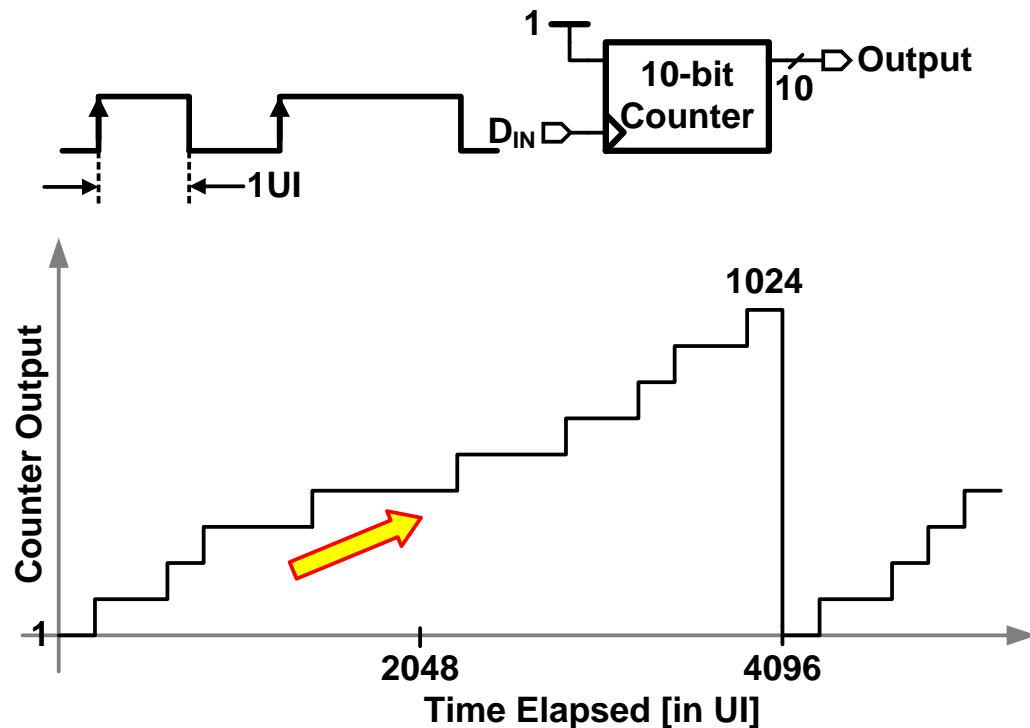
- ❑ Rotational frequency detector^[22-24]
- ❑ Quadri-correlator frequency detector^[25-26]
- ❑ Stochastic reference clock generator^[27]
- ❑ Miscellaneous FDs
 - Strobed linear PD^[27]
 - Counting based FDs^[28-29]

Accumulation – Alternating Data

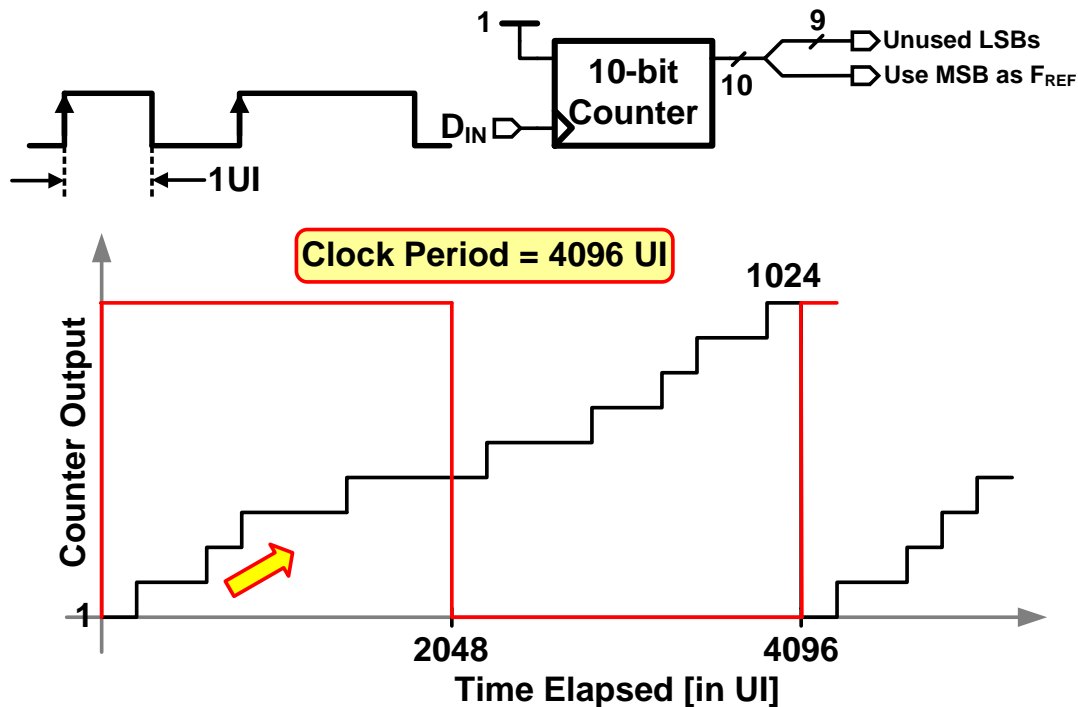


- ❑ Accumulator rolls over after 2048 UI

Accumulation – Random Data

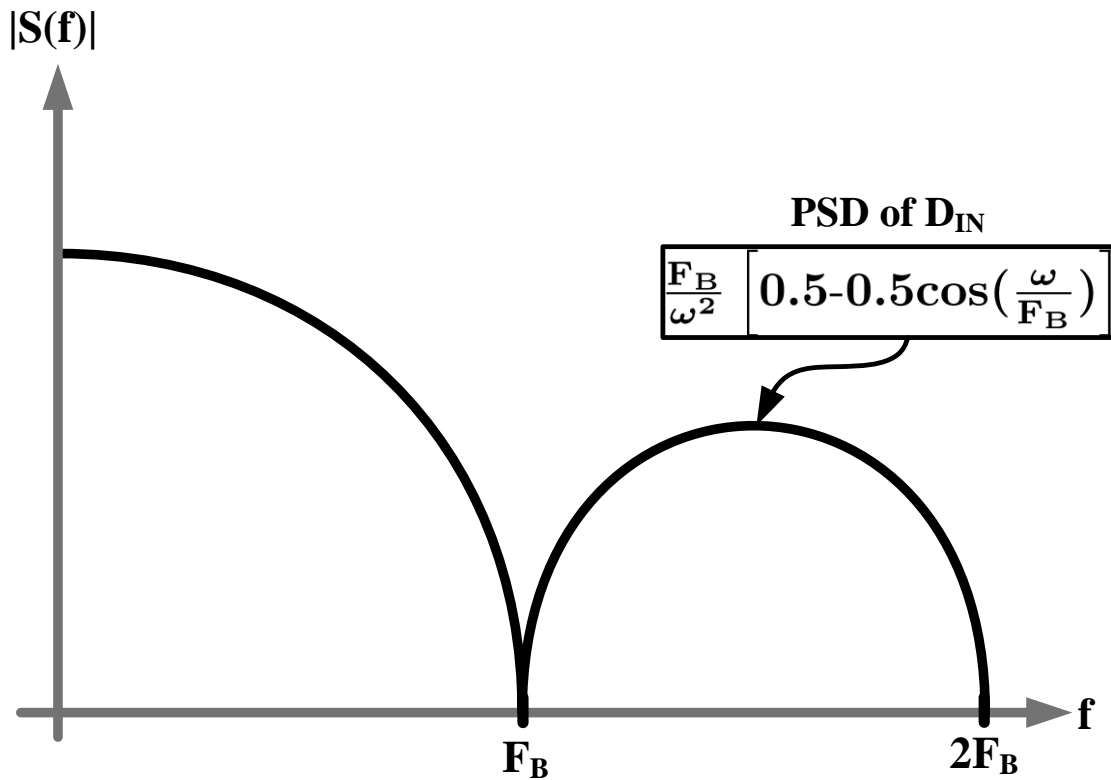


Extracting Clock from Counter Output



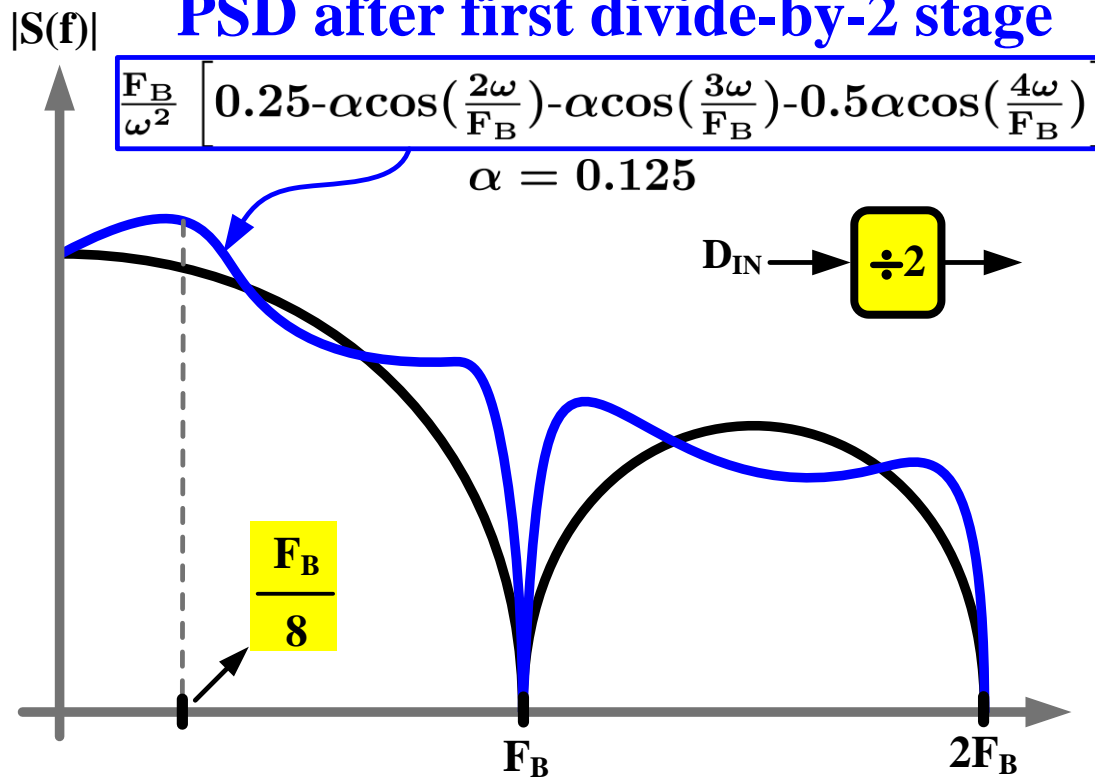
- ❑ MSB can be used for ref. clock w/ $1/F_{REF}=4096UI$

PSD of NRZ Random Data

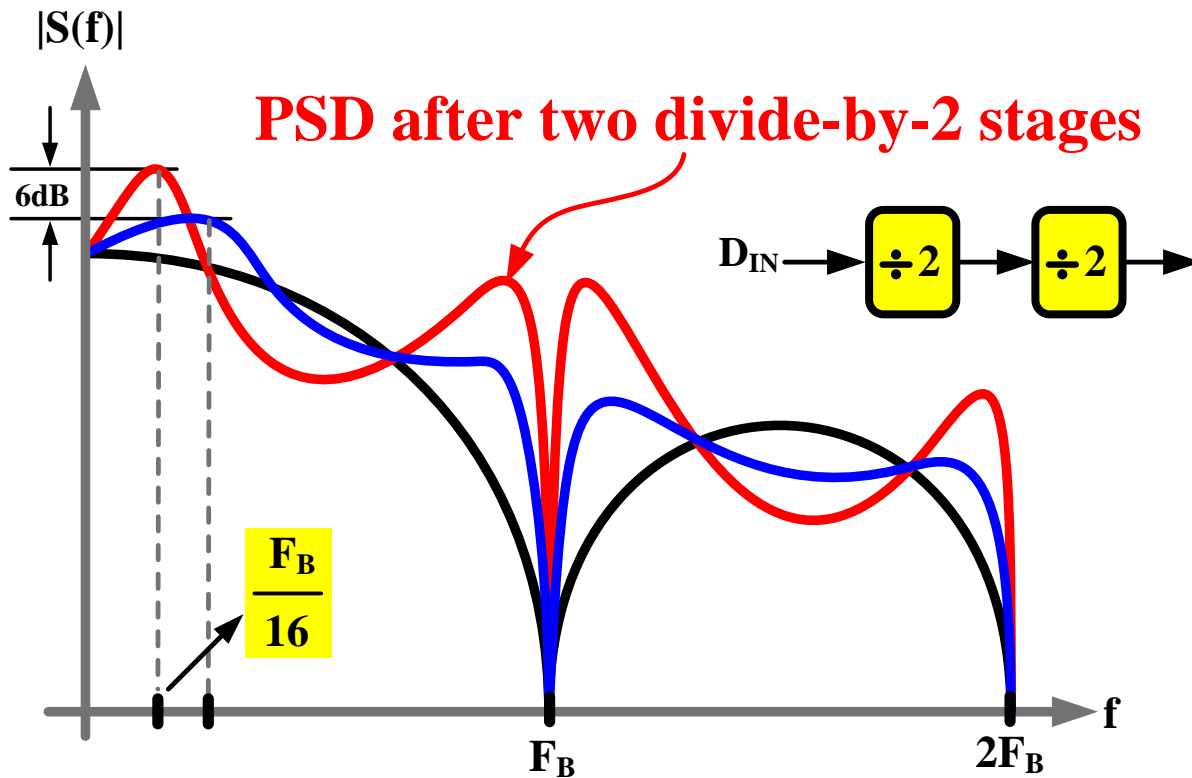


PSD After First Divide-by-2 Stage

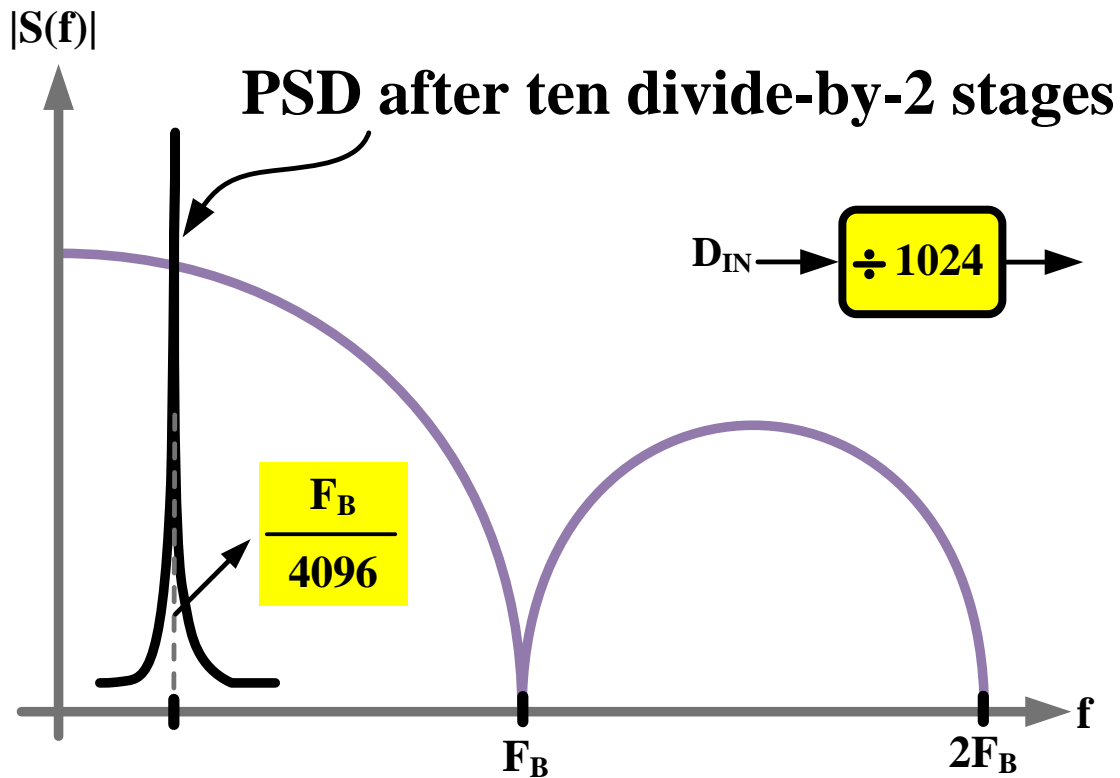
PSD after first divide-by-2 stage



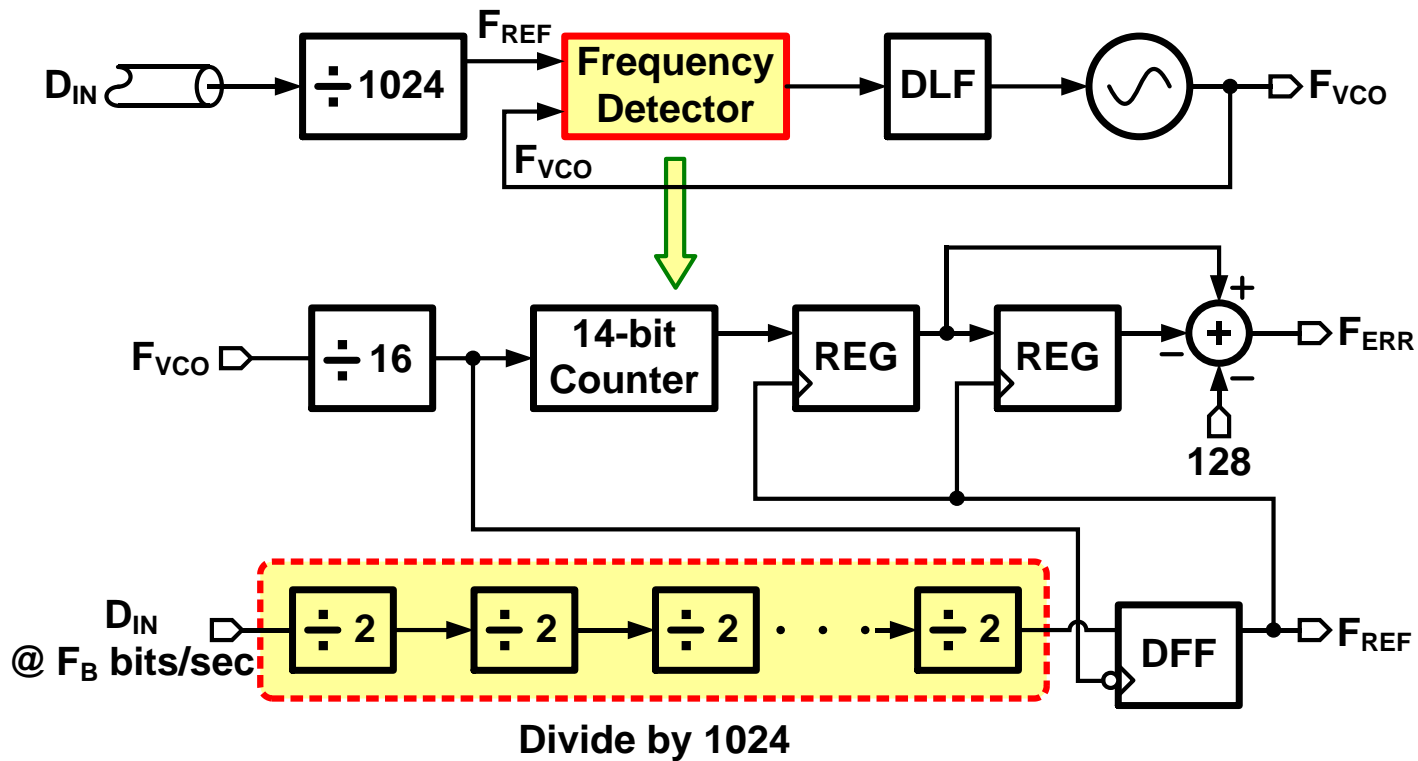
PSD After Two Divide-by-2 Stages



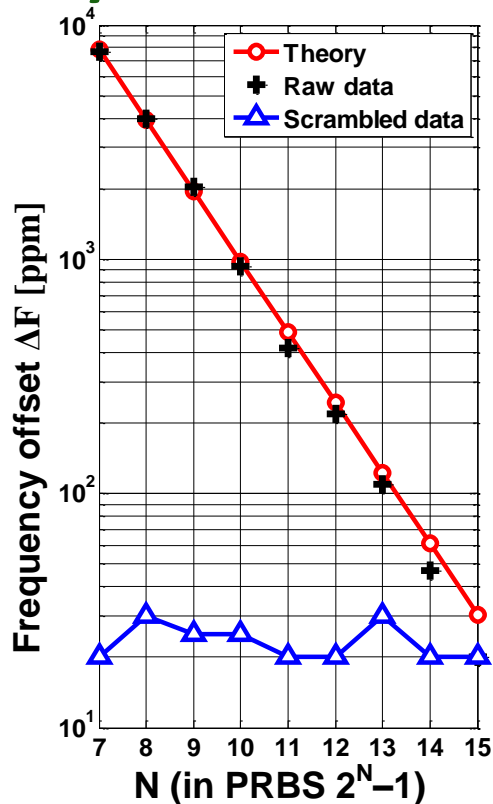
PSD After Ten Divide-by-2 stages



Frequency Locking Loop^[28]



FLL only Mode

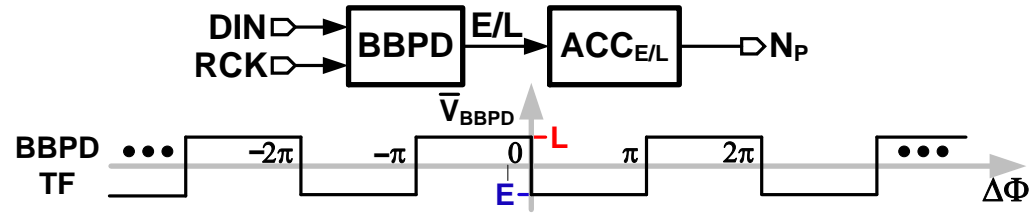


- PRBS patterns have *imbalance* in the $1 \rightarrow 0, 0 \rightarrow 1$ transitions

$$\text{Theoretical } \Delta F \text{ [ppm]} \approx \frac{10^6}{2^N}$$

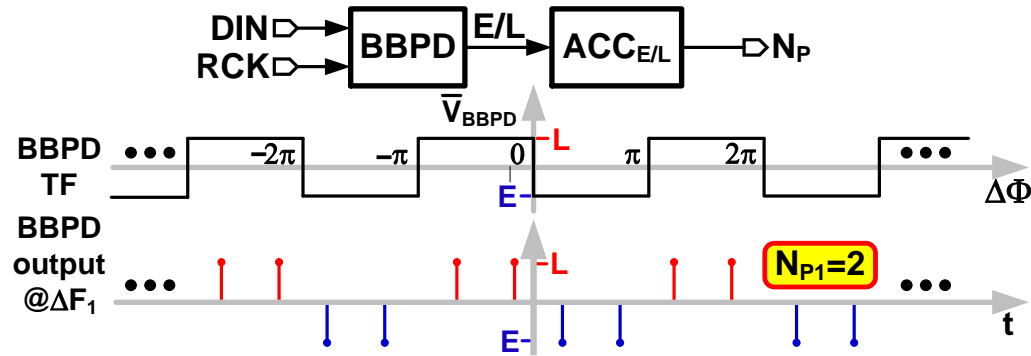
- Ex: PRBS7 imbalance = $1/127$
- Improved by scrambling

Principle of Frequency Detection_{1/4}



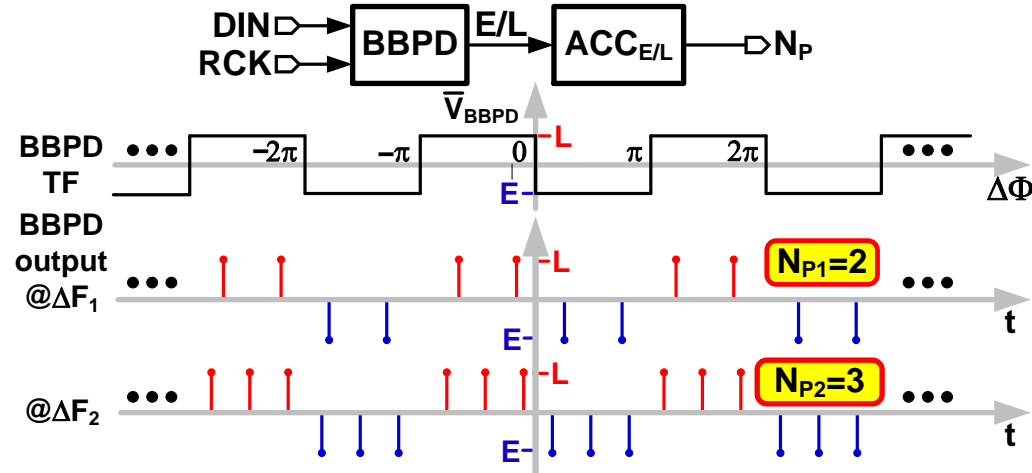
□ BBPD output changes sign at $\Delta\Phi = n\pi$

Principle of Frequency Detection_{2/4}



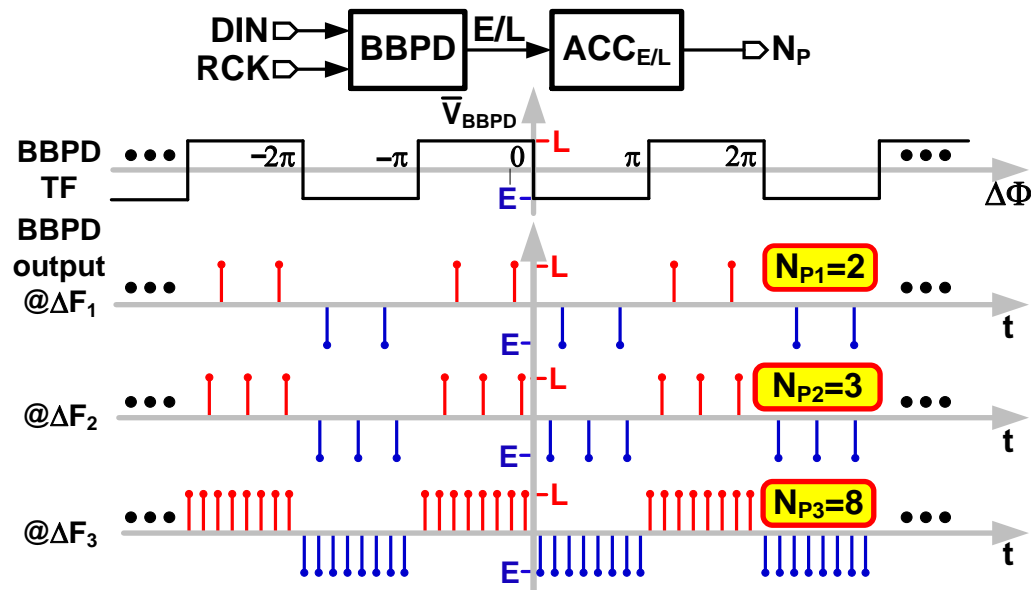
□ N_P is consecutive Early or Late number in π interval

Principle of Frequency Detection_{3/4}



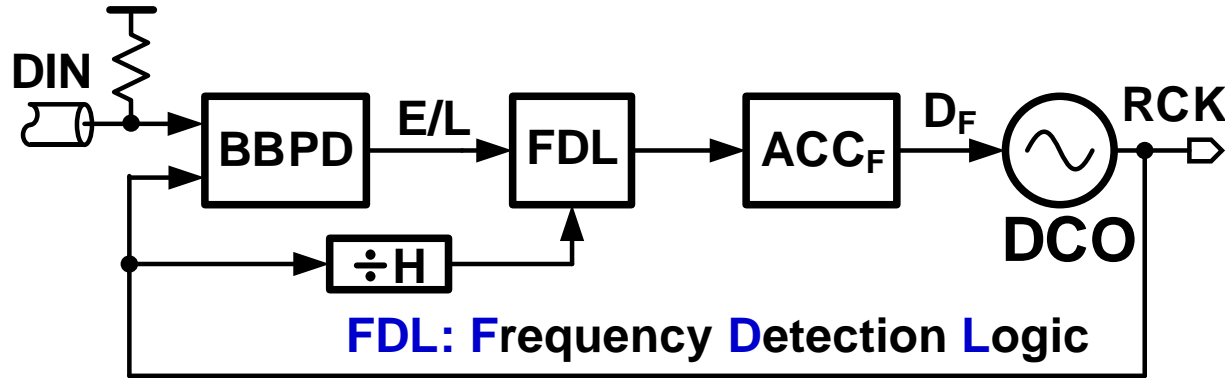
$\Delta F_2 < \Delta F_1$ leads to $N_{P2} > N_{P1}$

Principle of Frequency Detection_{4/4}



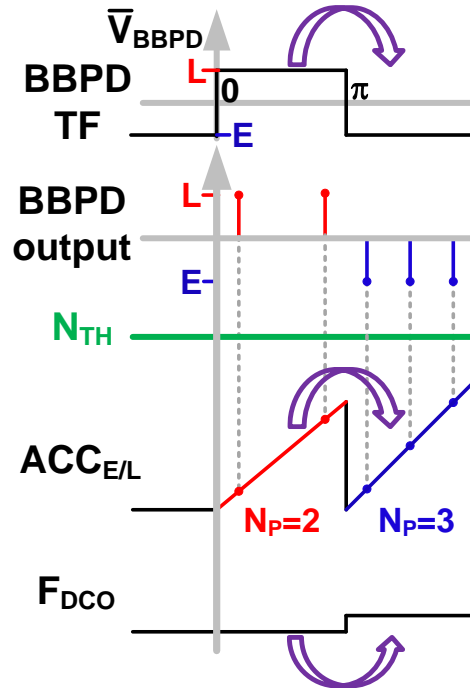
$\Delta F \propto 1/N_P \rightarrow$ Can be used for frequency detection

BBPD-based Frequency-Locked Loop^[29]



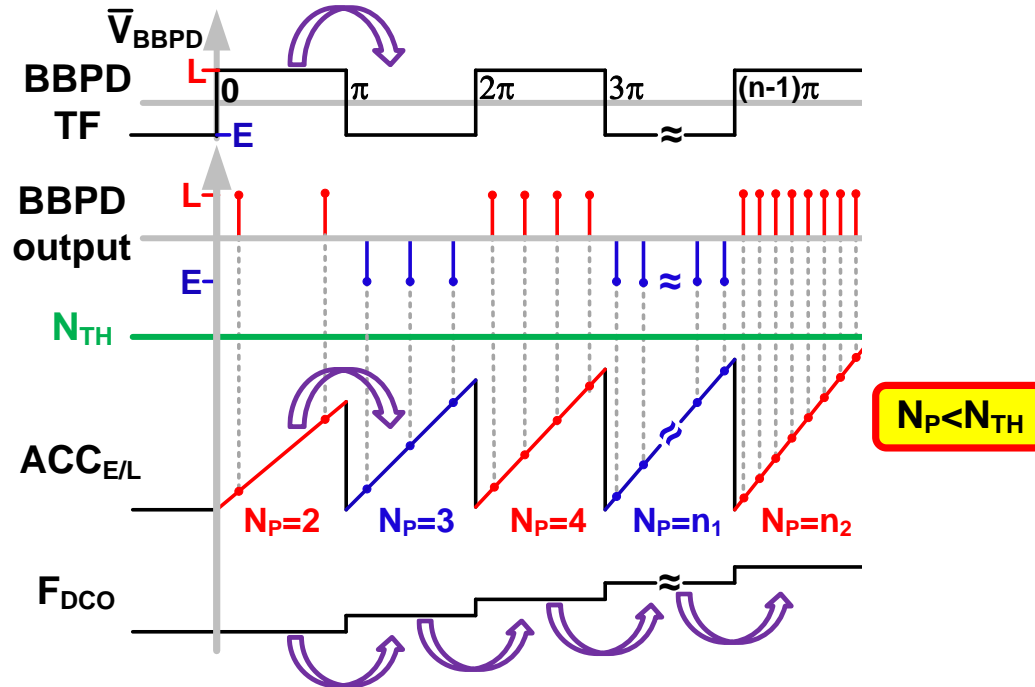
- ❑ No explicit frequency detector
- ❑ Immune to input transition density ρ
- ❑ Unlimited frequency acquisition range

Frequency Acquisition Process_{1/3}



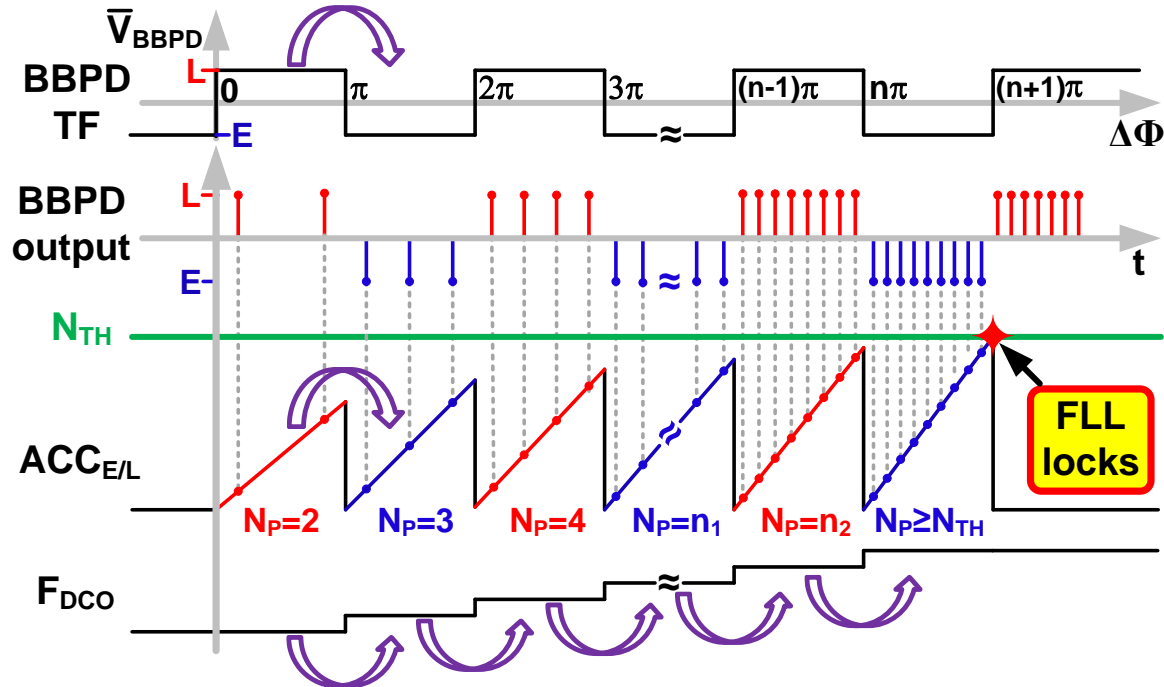
DCO starts from its lowest frequency

Frequency Acquisition Process_{2/3}



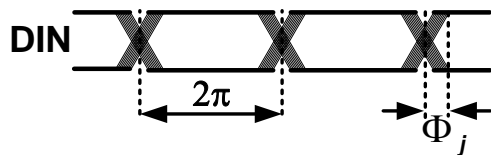
Increment F_{DCO} at each $E \rightarrow L$ or $L \rightarrow E$ transition

Frequency Acquisition Process_{3/3}



Lock is achieved when $N_p \geq N_{TH}$

Transition Density Dependence w/ Jitter



$$N_{TH} = N_P = \rho \frac{F_{DIN}}{\Delta F} \frac{\pi - \Phi_j}{2\pi}$$

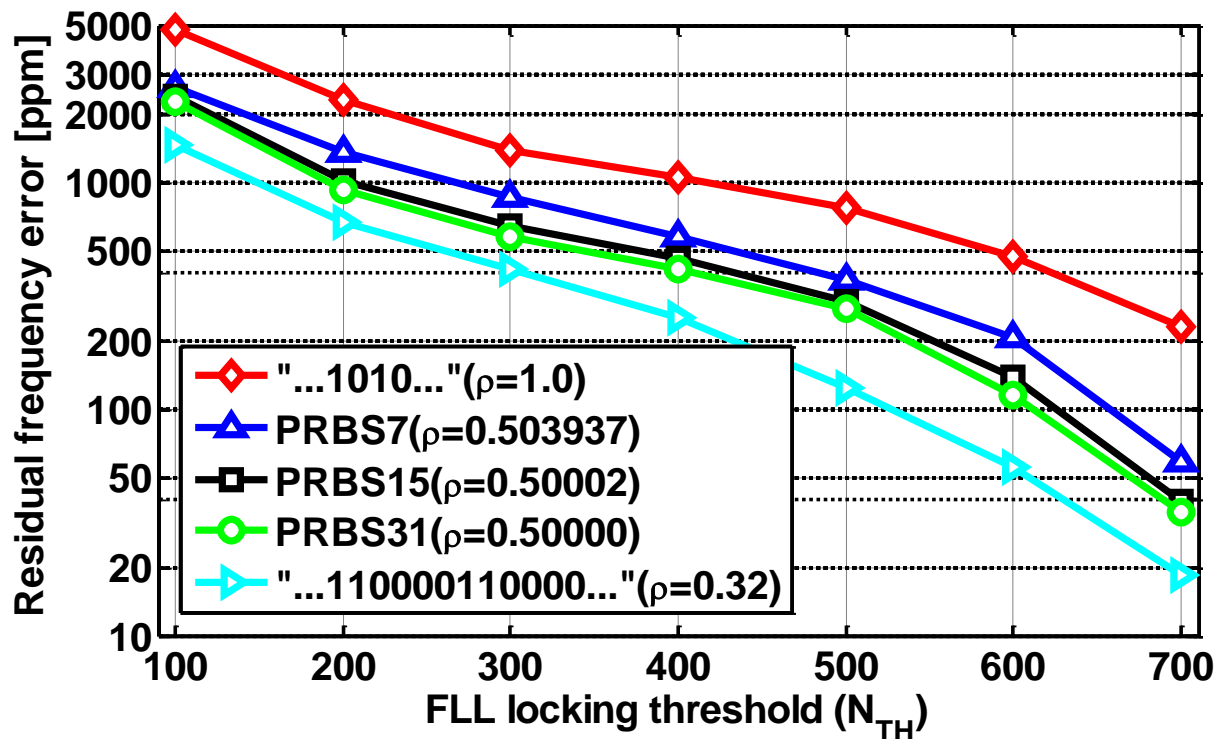
$$\Rightarrow \frac{\Delta F}{F_{DIN}} = \frac{\rho}{N_P} \frac{\pi - \Phi_j}{2\pi}$$

$N_{TH} = 500$

ρ	0.1	0.5	1.0
$\Phi_j=0$ $\Delta F/F_{DIN}$ [ppm]	100	500	1000
$\Phi_j=\pi/4$ $\Delta F/F_{DIN}$ [ppm]	75	375	750

$N_{TH}=N_P=500, \Delta F < 1000\text{ppm}$ when $0 \leq \rho \leq 1$

Residual Frequency Error



□ $N_{TH} \geq 500$, residual frequency error within 1000ppm

Summary

- ❑ Basic analog/digital clock and data recovery design for given jitter metrics
- ❑ Benefits analog and digital CDRs are exploited in hybrid analog/digital CDRs
- ❑ Multi-lane CDRs with local sampling clock & global low jitter recovered clock
- ❑ CDRs in repeaters with decoupled JTRAN & JTOL bandwidth
- ❑ FDs with simple counting of received signal transitions or !!PD outputs

Selected References

1. C. Hogge, "A self correcting clock recovery circuit," *J. Lightwave Technol.*, pp. 1312-1314, Dec. 1985.
2. L. DeVito, "A versatile clock recovery architecture and monolithic implementation," in *Monolithic Phase-Locked Loops and Clock Recovery Circuits*, B. Razavi, Ed. Wiley-IEEE Press, 1996, pp. 405-420.
3. J. Alexander, "Clock recovery from random binary signals," *Electr. Lett.*, pp. 541-542, Oct. 1975.
4. J. Lee and B. Razavi, "Analysis and modeling of bang-bang clock and data recovery circuits," *IEEE J. Solid-State Circuits*, pp. 1571-1580, Sep. 2004.
5. R. Walker, et al., "A 2-Chip 1.5 Gigabaud serial link interface," *IEEE J. Solid-State Circuits*, pp. 1805-1811, Dec. 1992.
6. J. Sonntag and J. Stonick "A digital clock and data recovery architecture for multi-gigabit/s binary links", *IEEE J. Solid-State Circuits*, pp.1867-1875, Aug. 2006.
7. M. Talegaonkar, R. Inti, P. Hanumolu, "Digital clock and data recovery circuit design: Challenges and tradeoffs", *IEEE Custom Integrated Circuits Conference*, 2011.
8. W. Yin, R. Inti, A. Elshazly, and P. Hanumolu, "A TDC-less 7mW 2.5Gb/s digital CDR with linear loop dynamics and offset-free data recovery," in *ISSCC Dig. Tech. Papers*, pp. 440-442, Feb. 2011.
9. S. Sidiropoulos and M. Horowitz, "A semidigital dual delay-locked loop," *IEEE J. Solid-State Circuits*, 1683–1692, 1997.

Selected References

10. M. Y. He and J. Poulton, "A CMOS mixed-signal clock and data recovery circuit for OIF CEI-6G+ backplane transceiver," *IEEE J. Solid-State Circuits*, vol. 41, no. 3, pp. 597–606, Mar. 2006.
11. B. Raghavan *et al.*, "A sub-2W 39.8-to-44.6Gb/s transmitter and receiver chipset with SFI-5.2 interface in 40nm CMOS," in *IEEE Int. Solid-State Circuits Conf. (ISSCC) Dig. Tech. Papers*, Feb. 2013, pp. 32–33.
12. U. Singh *et al.*, "A 780mW 4×28Gb/s transceiver for 100GbE gearbox PHY in 40nm CMOS," in *IEEE Int. Solid-State Circuits Conf. (ISSCC) Dig. Tech. Papers*, Feb. 2014, pp. 40–41.
13. P. Upadhyaya *et al.*, "A 0.5-to-32.75Gb/s flexible-reach wireline transceiver in 20nm CMOS," in *IEEE Int. Solid-State Circuits Conf. (ISSCC) Dig. Tech. Papers*, Feb. 2015, pp. 1–3.
14. S. Saxena, *et al.*, "A 2.8 mW/Gb/s, 14 Gb/s Serial Link Transceiver," *IEEE J. Solid-State Circuits*, vol. 52, no. 5, pp. 1399–1411, May 2017.
15. T. Lee and J. Bulzacchelli, "A 155-MHz clock recovery delay-and phase-locked loop," *IEEE J. Solid-State Circuits*, pp. 1736–1746, Dec. 1992.
16. J. Kenney, *et al.*, "A 9.95–11.3-Gb/s XFP transceiver in 0.13- μ m CMOS," *IEEE J. Solid-State Circuits*, vol. 41, no. 12, pp. 2901–2910, Dec. 2006.

Selected References

17. T. Toifl, *et al.*, “A 0.94-ps-RMS-Jitter 0.016-mm² 2.5-GHz multiphase generator PLL with 360 degree digitally programmable phase shift for 10-Gb/s serial links,” *IEEE J. Solid-State Circuits*, vol. 40, no. 12, pp. 2700–2712, Dec. 2005.
18. T. Toifl, *et al.*, “A 72-mW 0.03-mm² inductorless 40-Gb/s CDR in 65-nm SOI CMOS,” in *IEEE ISSCC Dig. Tech. Papers*, Feb. 2007, vol. 38, pp. 226–228.
19. W. Yin, *et al.*, “A 0.7-to-3.5-GHz 0.6-to-2.8-mW highly digital phase-locked loop with bandwidth tracking,” *IEEE J. Solid-State Circuits*, vol. 46, no. 8, pp. 1870–1880, Aug. 2011.
20. D. Dalton *et al.*, “A 12.5-Mb/s to 2.7-Gb/s continuous-rate CDR with automatic frequency acquisition and data-rate readback,” *IEEE J. Solid-State Circuits*, vol. 40, no. 12, pp. 2713–2725, Dec. 2005.
21. J. Kenney *et al.*, “A 6.5-Mb/s to 11.3-Gb/s continuous-rate clock and data recovery,” in *Proc. IEEE Custom Integrated Circuits Conf. (CICC)*, Sep. 2014, pp. 1–4.
22. G. Shu *et al.*, “A reference-less clock and data recovery circuit using phase-rotating phase-locked loop,” *IEEE J. Solid-State Circuits*, vol. 49, no. 4, pp. 1036–1047, Apr. 2014.
23. G. Shu, *et al.*, “A 4-to-10.5-Gb/s continuous-rate digital clock and data recovery with automatic frequency acquisition,” *IEEE J. Solid-State Circuits*, vol. 51, no. 2, pp. 428–439, Feb. 2016.

Selected References

- 22. D. Richman, "Color-Carrier Reference Phase Synchronization Accuracy in NTSC Color Television," *Proceedings of the IRE*, vol. 42, no.1, pp.106-133, Jan. 1954.
- 23. A. Pottbacker, et al., "A Si bipolar phase and frequency detector IC for clock extraction up to 8 Gb/s," *IEEE J. Solid-State Circuits*, pp.1747,1751, Dec 1992
- 24. D. Dalton, et al., "A 12.5-Mb/s to 2.7-Gb/s continuous-rate CDR with automatic frequency acquisition and data-rate readback," *IEEE J. Solid-State Circuits*, pp. 2713–2725, Dec. 2005.
- 25. F. M. Gardner, "Properties of frequency difference detectors," *IEEE Trans. Comm.*, vol. COM-36, no. 2, pp. 131–138, Feb. 1985.
- 26. N. Kocaman, et al., "An 8.5–11.5-Gbps SONET transceiver With reference-less frequency acquisition," *IEEE J. Solid-State Circuits*, pp. 1875–1884, Aug. 2013.
- 27. S. Huang, et al., "An 8.2-to-10.3 Gb/s full-rate linear reference-less CDR without frequency detector in 0.18 μ m CMOS," in *IEEE ISSCC Dig. Tech. Papers*, Feb 2014, pp. 152–153.
- 28. R. Inti, et al., "A 0.5-to-2.5 Gb/s reference-less half-rate digital CDR with unlimited frequency acquisition range and improved input duty-cycle error tolerance," *IEEE J. Solid-State Circuits*, pp. 3150–3162, Dec. 2011.
- 29. G. Shu, et al., "A 4-to-10.5 Gb/s 2.2 mW/Gb/s continuous-rate digital CDR with automatic frequency acquisition in 65 nm CMOS," in *IEEE ISSCC Dig. Tech. Papers*, Feb 2014, pp. 150–151.

